

**NUMERICAL SIMULATIONS AND AN EXPERIMENTAL
INVESTIGATION OF A FINGER SEAL**

Minel Braun, Hazel Pierson, H. Li, and Dingeng Dong
University of Akron
Akron, Ohio



**2005 NASA/Seal Secondary Air System
Workshop
At Ohio Aerospace Institute
November 8-9, 2005**



**NUMERICAL SIMULATIONS AND
AN EXPERIMENTAL
INVESTIGATION OF A FINGER
SEAL**

M.J. Braun*
H.M. Pierson, H. Li, D. Deng

**Dept. of Mechanical Engineering,
University of Akron, Akron, OH 44325, USA**
**(*) Corresponding author: Tel: 330-972-7734; email:
mjbraun@uakron.edu**



ACKNOWLEDGEMENT

Advanced
Technology

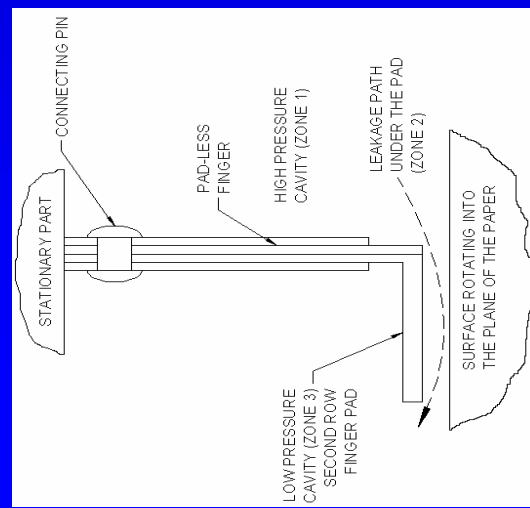


For Intelligent
Gas Turbines

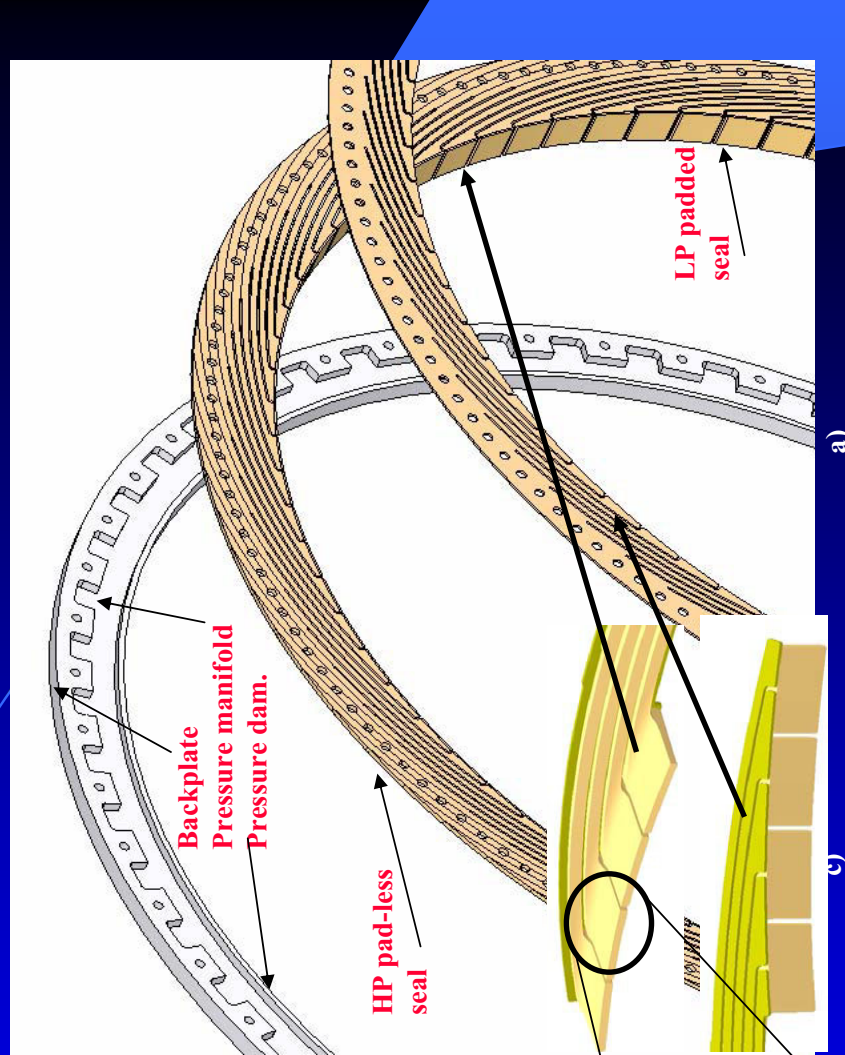
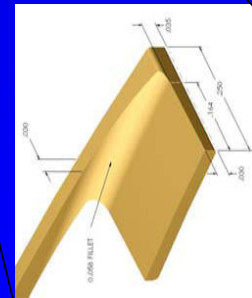
The authors want to express their gratitude to M. Proctor and B. Steinetz of NASA Glenn Research Center, Cleveland, Ohio for the financial support and technical consultations.

November 8, 2005

CONCEPT AND COMPONENTS



General Configuration



a)

c)

Full Wafer of Padded Fingers (8.5" ID, 9.666" OD, 81 Fingers) and details (b, c) of the Arrangement of the High and Low Pressure Fingers

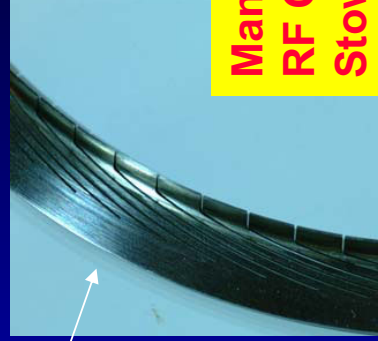
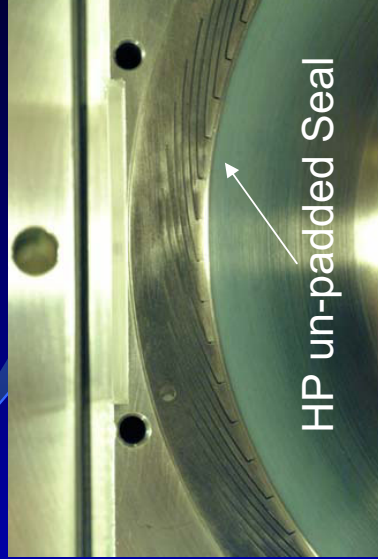
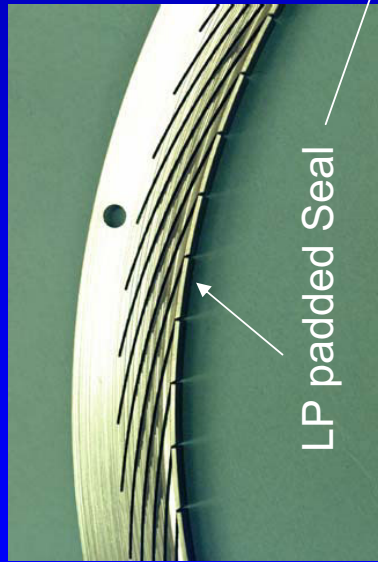
ACTUAL HARDWARE



Advanced
Technology



For Intelligent
Gas Turbines



Manufactured by:
RF Cook
Stow, OH 44224

Padded and Unpadded Sections of HP- and LP-seals

November 8, 2005



DESIGN PARAMETERS

(Variations in the Design of the Finger Stick and Foot)

Advanced
Technology



For Intelligent
Gas Turbines

Besides sealing, the other main goal of a successful finger seal design is to exhibit appropriate compliance to outside forces. The ability of the seal to ride or float along the rotor without rubbing or excessive heating is essential to the successful operation of the seal.

The compliance of the finger must only occur in the radial plane;

The seal needs to be as sturdy as possible in the axial direction.

The compliant finger that moves radially outward with rotor growth and motion has to be able to ride the rotor back down as the rotor diameter recovers or the rotor moves “away”.

Thus there is an optimum stiffness for the finger;

November 8, 2005



DESIGN PARAMETERS (cont'd)

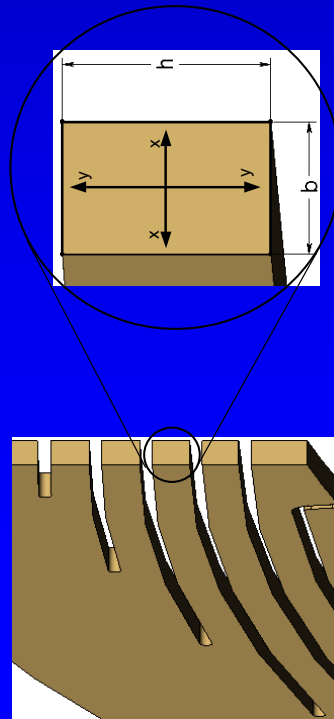
(Variations in the Design of the Finger Stick and Foot)

Advanced
Technology



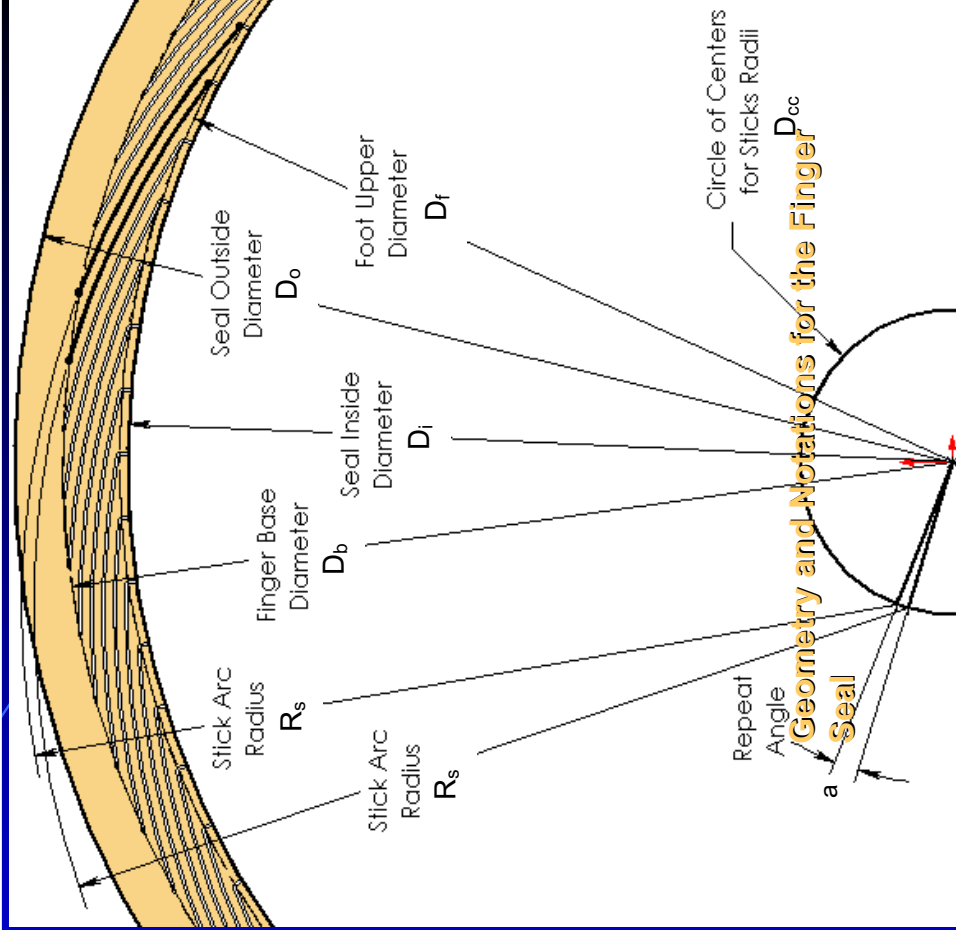
For Intelligent
Gas Turbines

- (1) D_{cc} Stick Arcs Circle of Centers.
- (2) R_s Stick Arc Radius.
- (3) D_b Finger Base Diameter.
- (4) D_f Foot Upper Diameter.
- (5) 'a' Finger Repeat Angle.
- (6) I_s Finger Interspace Width.
- (7) L_c Circumferential Foot Length.
- (8) 'b'-Laminate thickness.



View of Finger Stick Cross-Section

November 8, 2005





DESIGN PARAMETERS (cont'd)

(Variations in the Design of the Finger Stick and Foot)

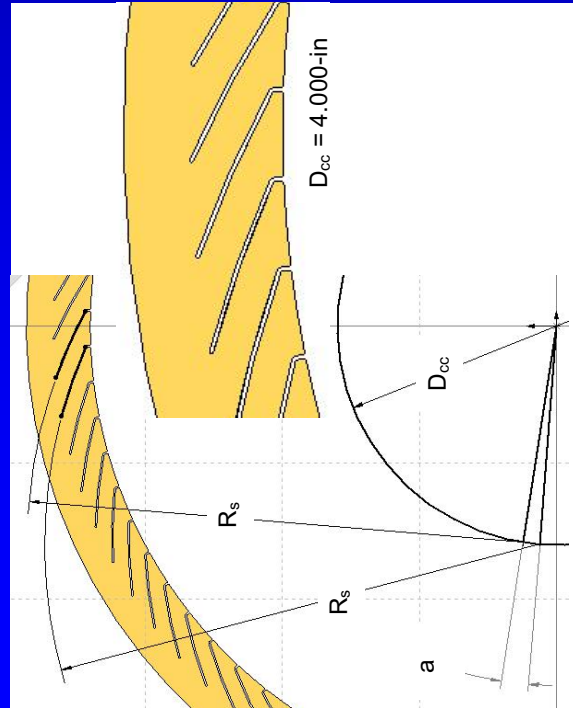
Advanced
Technology



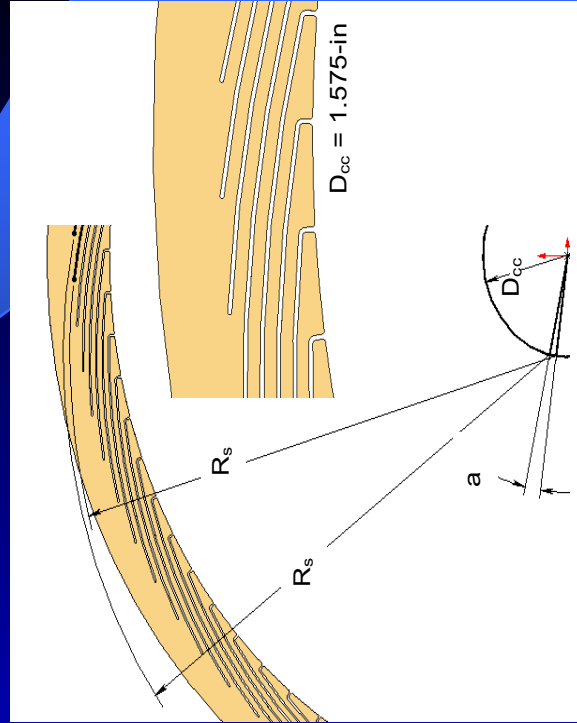
For Intelligent
Gas Turbines

1) D_{cc} Stick Arcs Circle of Centers

When the diameter of the circle of centers (D_{cc}) of the finger stick arcs was increased, while all other dimensions remained the same, the sticks became thicker and pointed more directly toward the center of the seal.



The two figures show the change in the shape of the finger stick when the circle of centers was increased to the diameter of (a) $D_{cc} = 4.000$ -in from (b) $D_{cc} = 1.575$ -in



November 8, 2005



DESIGN PARAMETERS (cont'd)

(Variations in the Design of the Finger Stick and Foot)

Advanced
Technology



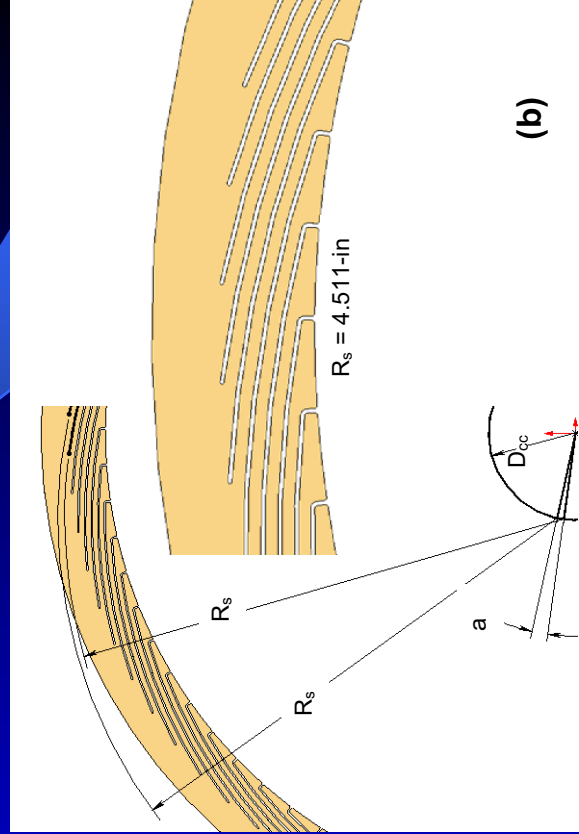
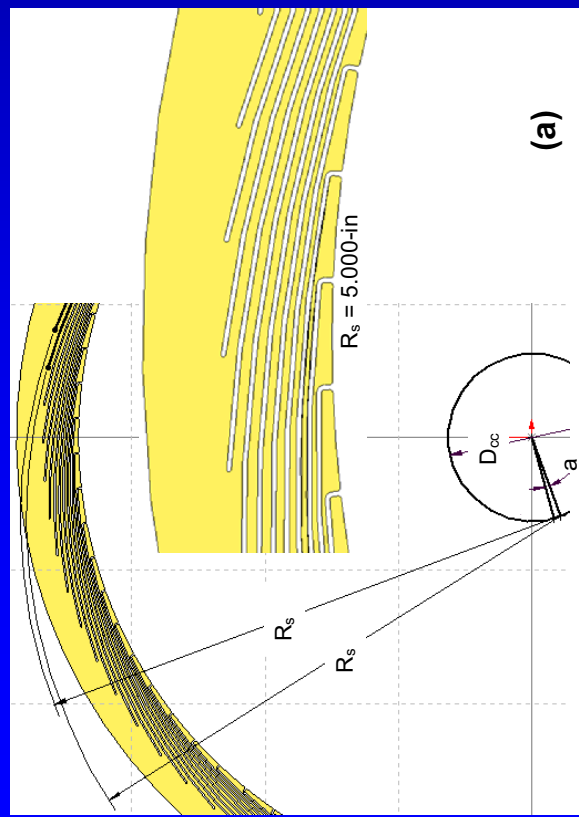
For Intelligent
Gas Turbines

(2) R_s Stick Arc Radius.

The two figures (a) and (b) show the change in the shape of the finger stick when the arc radius was increased to $R_s = 5.000$ -in from $R_s = 4.511$ -in.

NOTE:

The increase in R_s , while keeping D_{cc} constant, caused the sticks to curve more concentric with the inside diameter of the seal, and consequently make the stick length much longer.



November 8, 2005



DESIGN PARAMETERS (cont'd)

(Variations in the Design of the Finger Stick and Foot)

Advanced
Technology



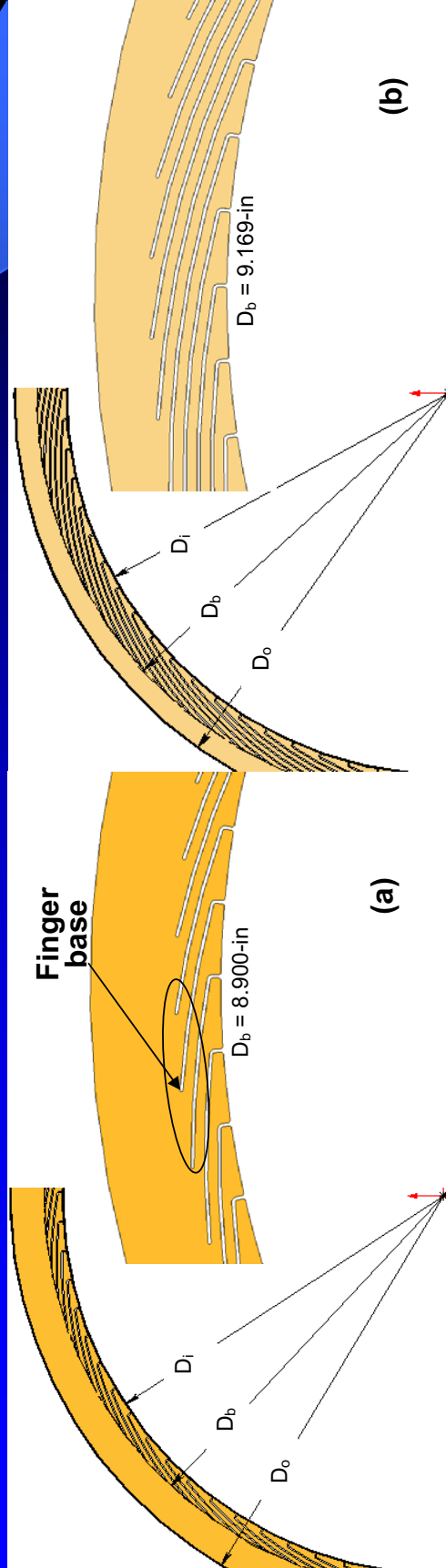
For Intelligent
Gas Turbines

(3) D_b Finger Base Diameter.

Figures (a) and (b) shows the seal in which the finger base diameter had been changed to (a) $D_b = 8.900$ -in. from (b) $D_b = 9.169$ -in.

NOTE:

When the finger base diameter, D_b , was changed, the stick length, L_{st} , changes. With all other dimensions kept constant, this variation only altered the length of the stick; the cross-sectional height, h , and the angle at which it attaches to the pad (foot) remained the same.



November 8, 2005



DESIGN PARAMETERS (cont'd)

(Variations in the Design of the Finger Stick and Foot)

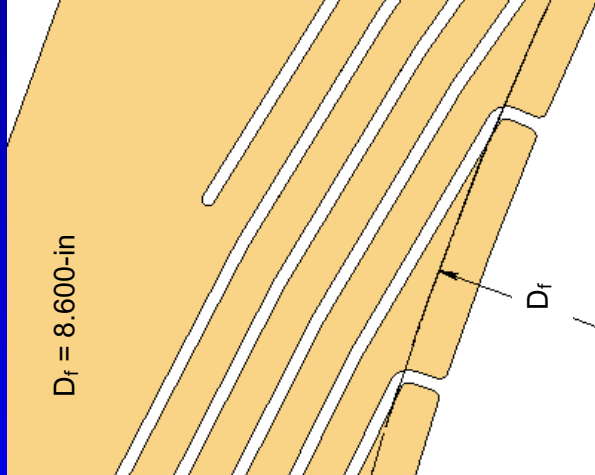
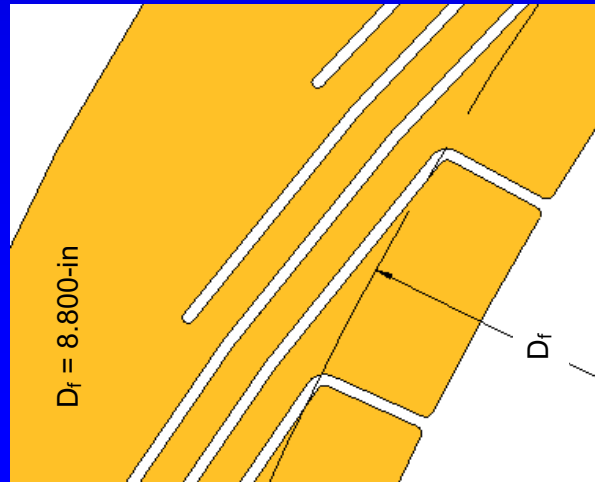
Advanced
Technology



For Intelligent
Gas Turbines

4) D_f Foot Upper Diameter.

Figures (a) and (b) shows the altered foot geometry as the upper foot diameter was changed to (a) $D_f = 8.800$ -in from (b) $D_f = 8.600$ -in. The mass of the foot can be altered by changing the upper foot diameter, D_f .



NOTE #1:

Altering the mass does not affect the equivalent stiffness of the finger, but it does have an impact on the finger dynamics.

increasing D_f also shortened the effective stick length, L_{st} , which significantly affects the finger stiffness.

NOTE #2:

D_b also affects the finger stiffness length L_{st} (see previous slide)

November 8, 2005



DESIGN PARAMETERS (cont'd)

(Variations in the Design of the Finger Stick and Foot)

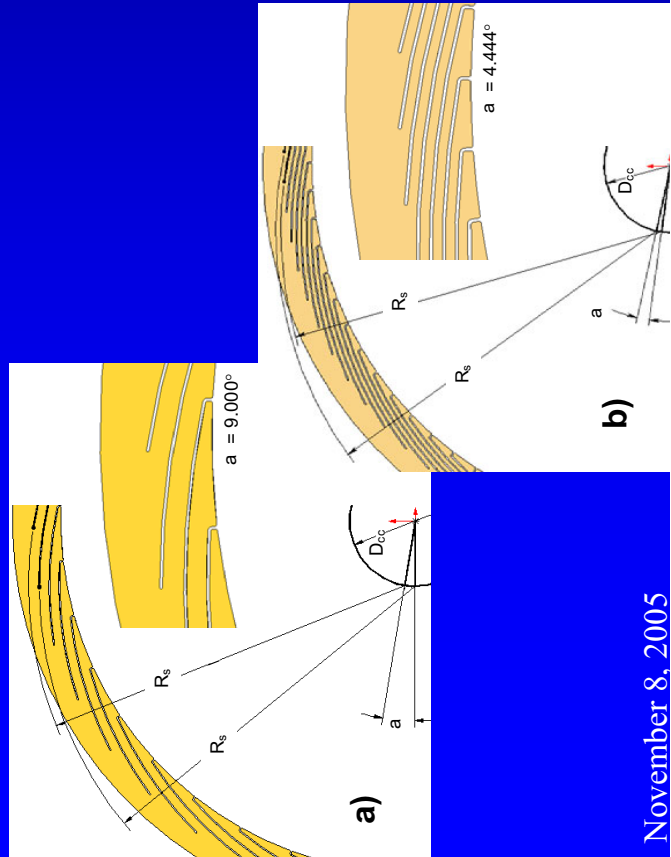
Advanced Technology



For Intelligent Gas Turbines

(5) 'a' Finger Repeat Angle.

Figures (a) and (b) shows the change to a 40 finger seal, (a) $a = 9.000^\circ$ repeat angle, from an 81 finger seal, (b) $a = 4.444^\circ$ repeat angle. It is the repeat angle, a , of the finger stick arcs that determines how many individual fingers will be in the total seal.



From the standpoint of the stick stiffness, the change in 'a' will cause a significant change in h ; doubling the height increased the area moment of inertia, and consequently the stiffness by eight fold, as summarized in the following Table for an increase in a to 9.000° .

| | Symbol | Original Value | Value change with the Increase of 'h' |
|------------------------|-------------|------------------------------------|---------------------------------------|
| Effective Stick Length | L_{st} | 1.6108-in | SAME |
| Cross-section Base | b | 0.030-in | SAME |
| Cross-section Height | h | 0.045-in | 0.090-in |
| Area Moment of Inertia | I_{xx} | $2.28 \times 10^{-7} \text{ in}^4$ | $1.822 \times 10^{-6} \text{ in}^4$ |
| Modulus of Elasticity | E | $31 \times 10^6 \text{ psi}$ | SAME |
| Stick Stiffness | k_{stick} | 5.07 - lbf/in | 40.55 - lbf/in |

November 8, 2005



DESIGN PARAMETERS (cont'd)

(Variations in the Design of the Finger Stick and Foot)

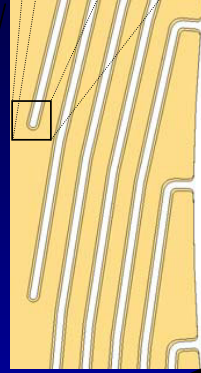
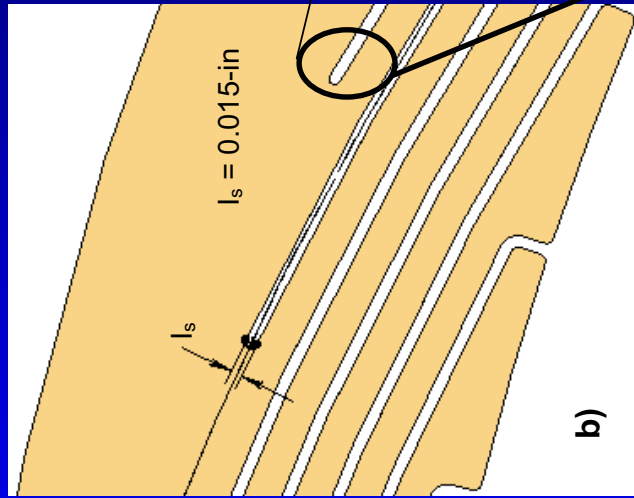
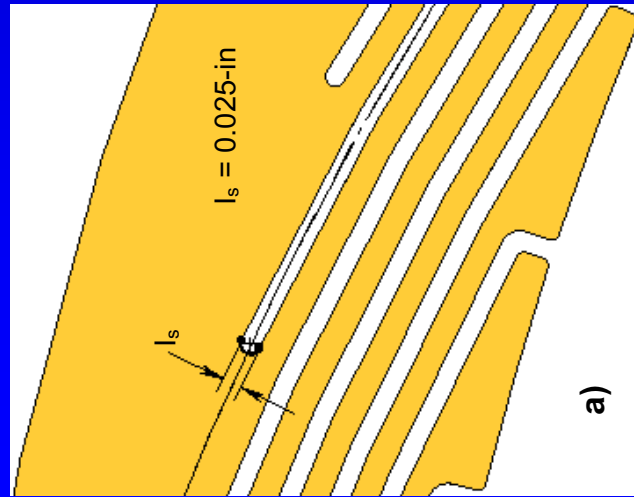
Advanced
Technology



For Intelligent
Gas Turbines

(6) I_s Finger Interspace Width

Figures (a) and (b) shows a finger seal with a change to an (a) $I_s = 0.025$ -in interspace from an (b) $I_s = 0.015$ -in interspace between fingers. The interspaces, I_s , (cutouts) between the individual fingers are what give the fingers the ability to move independently of each other.



Detail of interspace

NOTE:

The added space between the fingers allows the seal to open to a greater maximum diameter, but it also allows greater potential leakage.

Thus one has to optimize between freedom of movement and minimum leakage.

November 8, 2005



DESIGN PARAMETERS (cont'd)

(Variations in the Design of the Finger Stick and Foot)

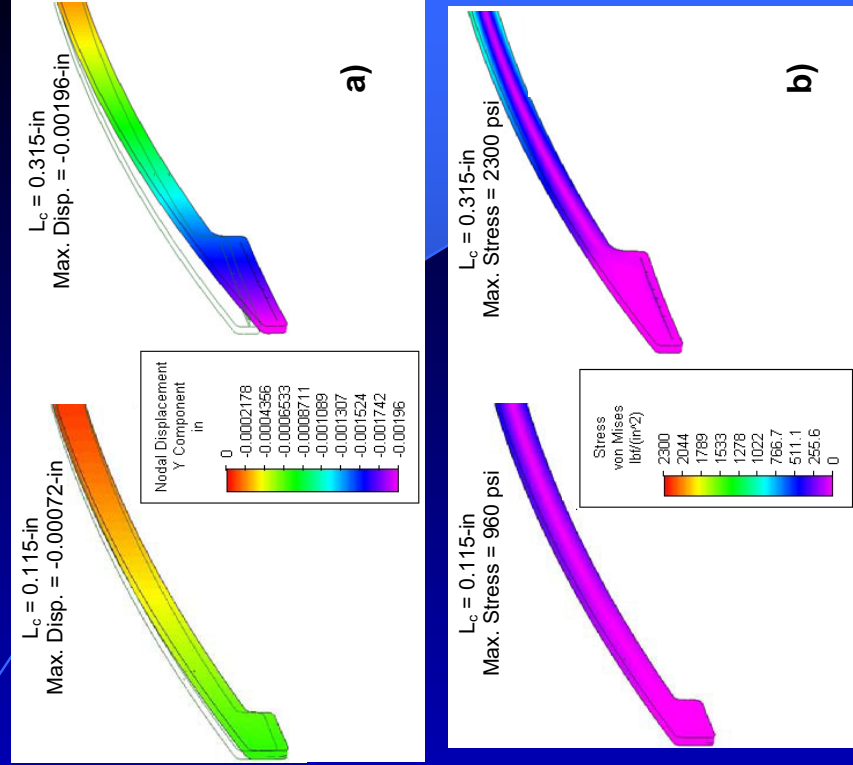
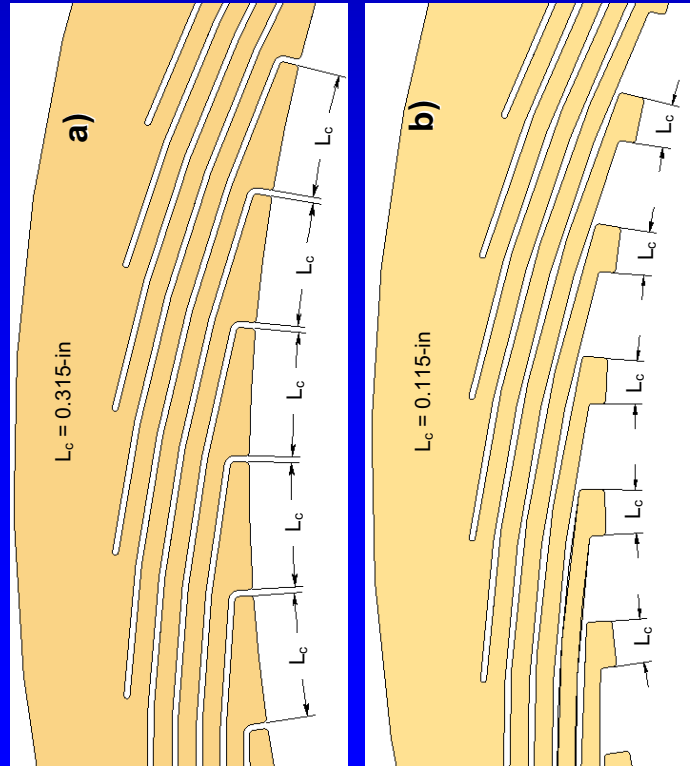
Advanced Technology



For Intelligent Gas Turbines

(7) L_c Circumferential Foot Length.

Figures (a) and (b) show a foot whose toe and heel were removed such that the arc length is reduced to (a) $L_c = 0.115$ -in from (b) $L_c = 0.315$ -in. Keeping all other parameters constant, the circumferential arc length, L_c , of the foot itself was considered for optimization



Resultant Contours Comparisons for a Change in L_c to 0.115-in from 0.315-in: (a) Deflection Dither, (b) Stress Dither

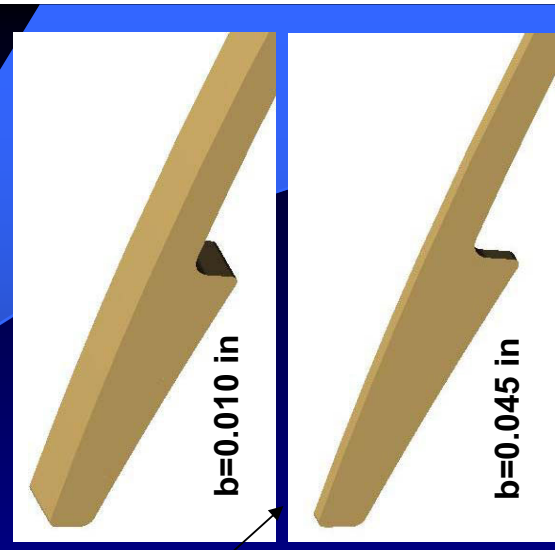
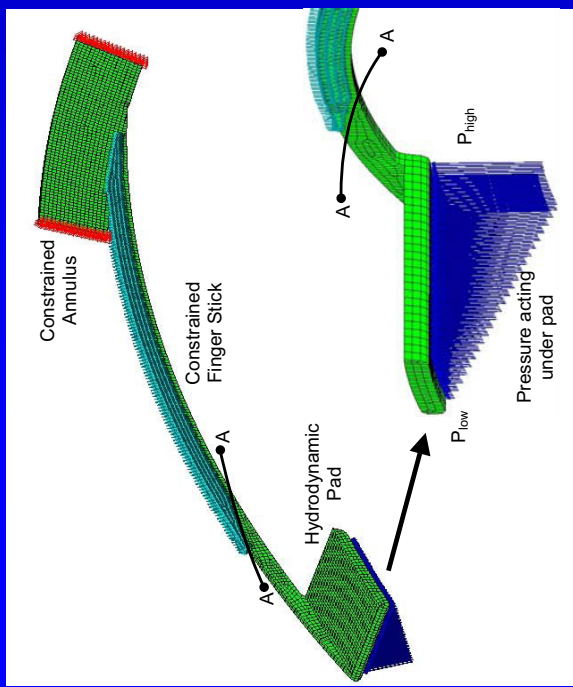
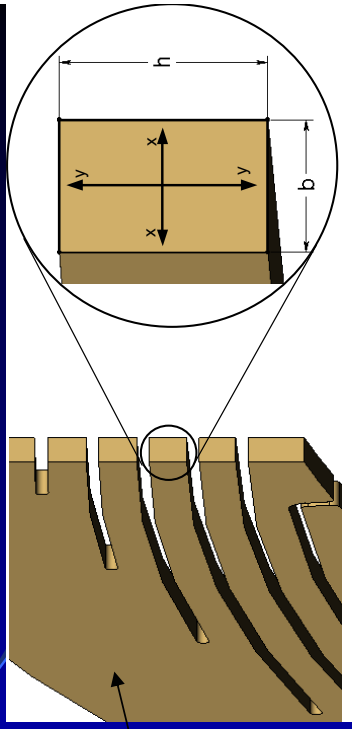
NOVEMBER 6, 2003



DESIGN PARAMETERS (cont'd)

(Variations in the Design of the Finger Stick and Foot)

(8) b-Laminate thickness.
 The final geometric variation of the finger portion that was evaluated was the cross-sectional thickness, b , of the individual finger laminates. Stiffness values, k_{stick} , were determined for a cross-sectional thickness ranges from $b = 0.010$ to $b = 0.045$.



FEM Loading and Boundary Conditions for Investigation of Finger Stick Twisting as a function of Finger Thickness, b



DESIGN PARAMETERS (cont'd)

(Variations in the Design of the Finger Stick and Foot)

Variations in Finger Pad Design

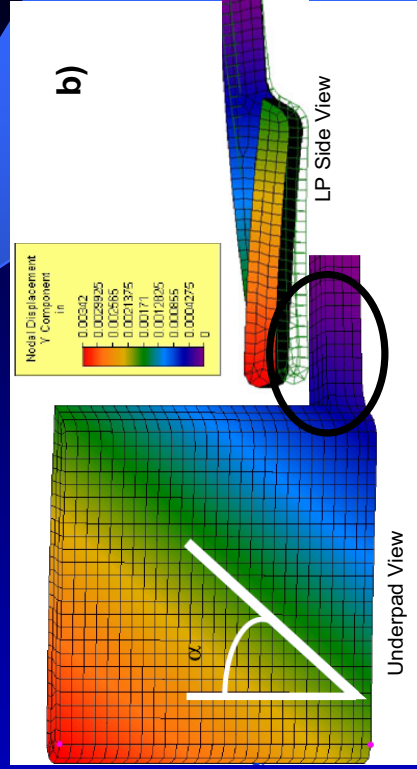
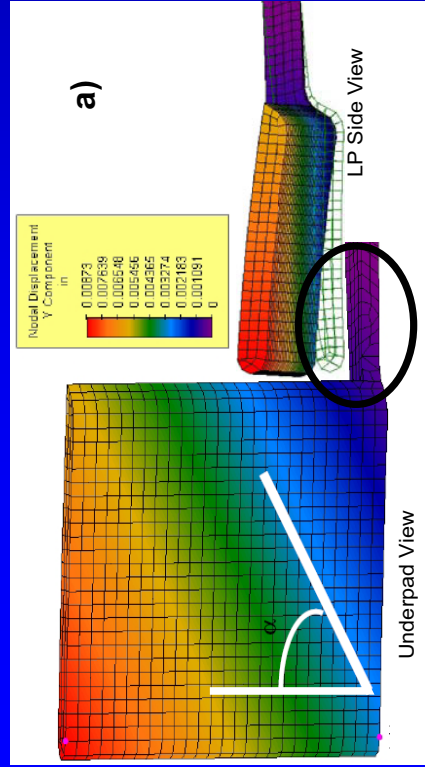
Advanced
Technology



For Intelligent
Gas Turbines

The finger seal obtains its hydrodynamic lifting capabilities from the pattern of the padded fingers underside, which “rides” the surface of the shaft. The objective in the design of the pad was to determine an optimal configuration that would enable the pad portion to lift from the rotating rotor and to run on a thin film of air during operation while minimizing the leakage rate

The desirable motion of the pad is one that is in sync with the motion of the stick while minimizing its rotation out-of-plane with respect to the stick. If the pad rotated around its heel, it could potentially both open the clearance for leakage and “dig” into the shaft at the origin of the pad rotation. Therefore the design of the pad had to minimize this situation.



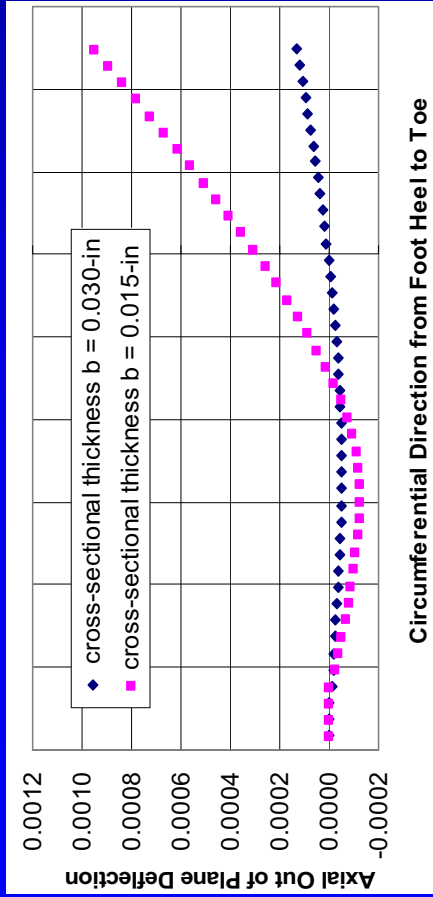
Radial Out-of-Plane Twisting as Viewed from Underneath the Pad and from the Low-Pressure Side: (a) Stick Thickness of $b=0.015$ -in, (b) Stick Thickness of $b=0.030$ -in

November 8, 2005

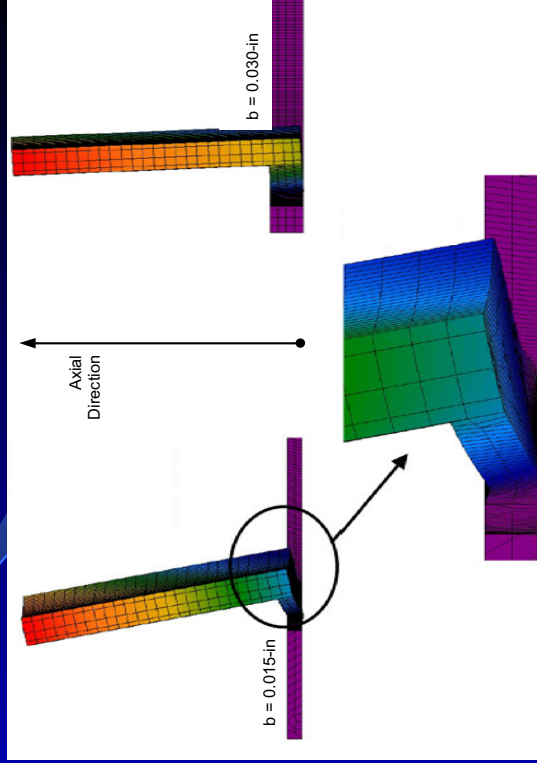
DESIGN PARAMETERS (cont'd)

(Variations in the Design of the Finger Stick and Foot)

Variations in Finger Pad Design



Shape of the underpad surface Axial Out-of-Plane Twisting for Stick Thickness of $b=0.015\text{-in}$ and $b=0.030\text{-in}$



Another view of pad and stick deformation



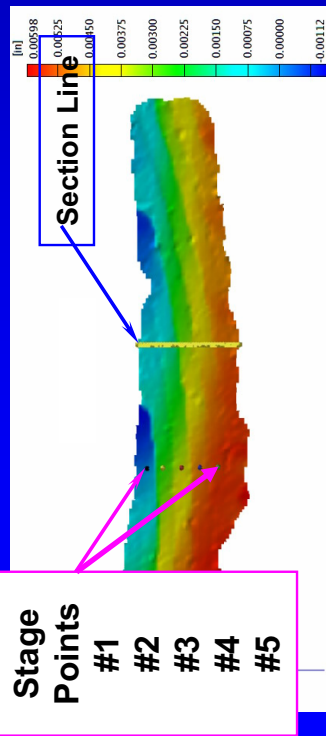
FINGER BEHAVIOR WITH ROTATING SHAFT AND AXIAL PRESSURE DIFFERENTIAL $\Delta p=5$ PSI

Advanced Technology



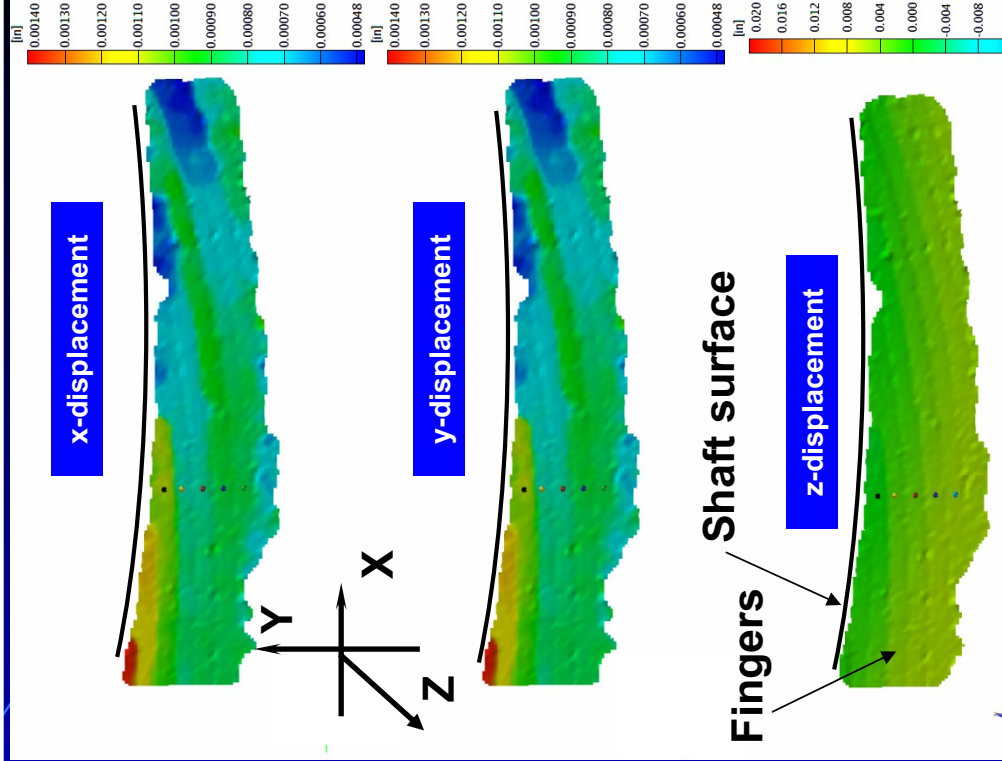
For Intelligent Gas Turbines

x-, y- and z- Displacements



Experimental Conditions:
 Rotation: 7000 RPM
 Axial pressure: 0 to 5 PSI

Photos of the fingers (the region shown in the above pictures) are taken by two cameras from different angles at the same time. The x (circumferential), y (radial), and z (axial) displacements are obtained by analyzing the pairs of the images.



NOVEMBER, 2000

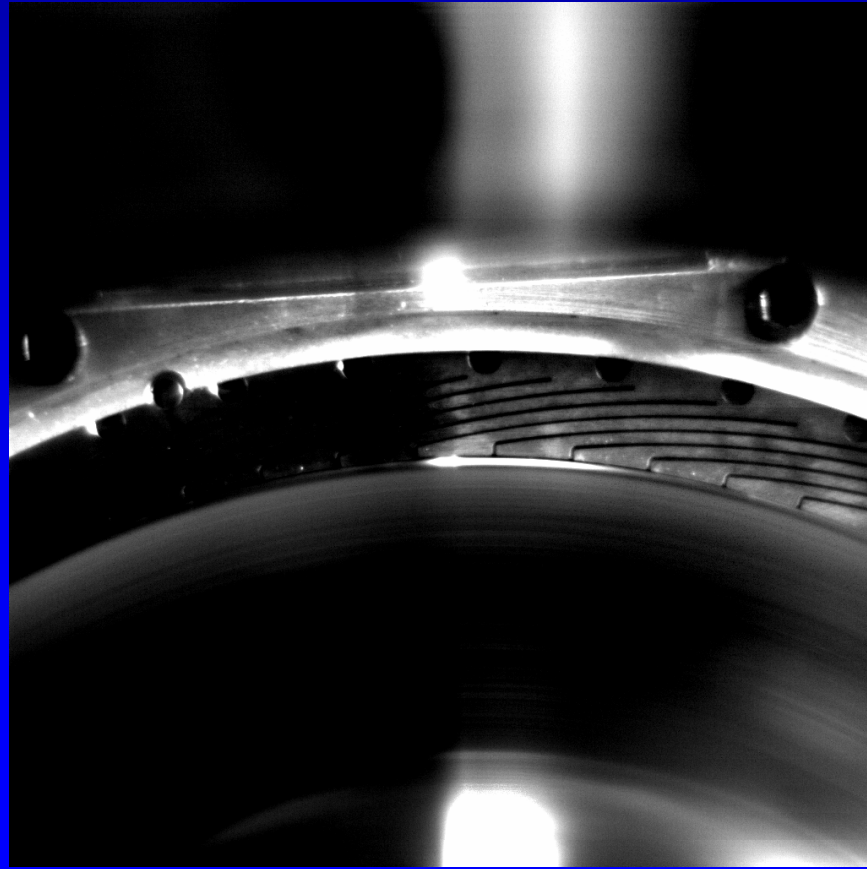


Fingers Motion and Deformation Animation

Advanced
Technology

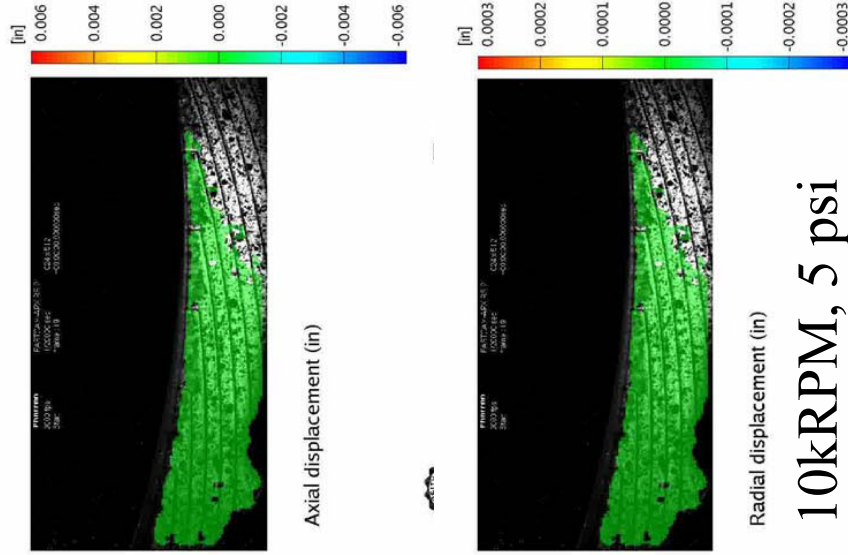


For Intelligent
Gas Turbines



10,000 RPM

November 8, 2005



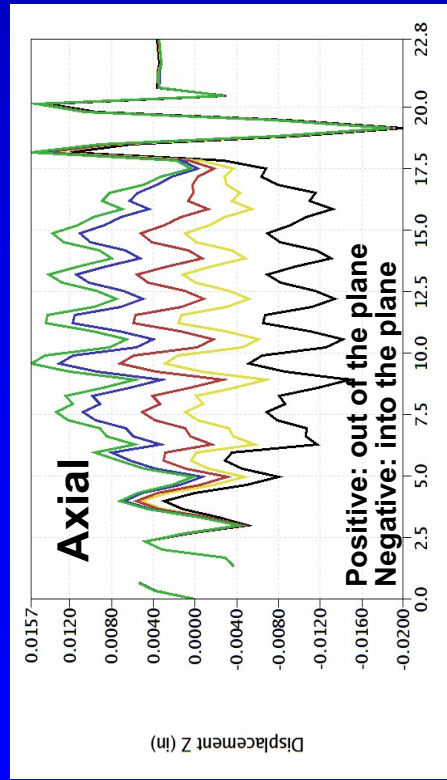
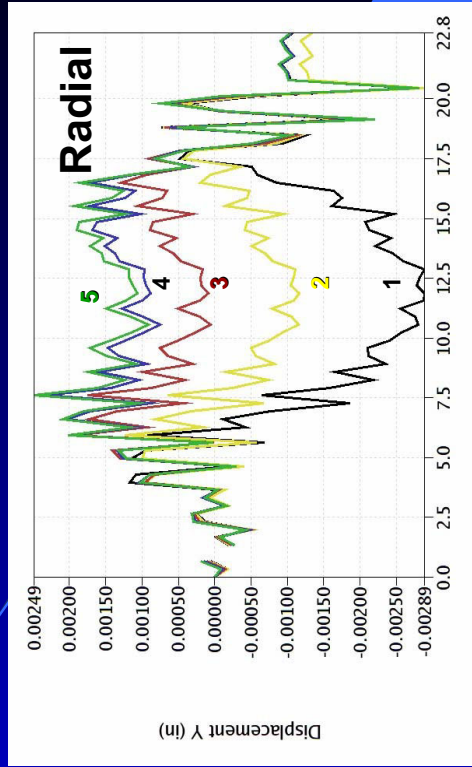
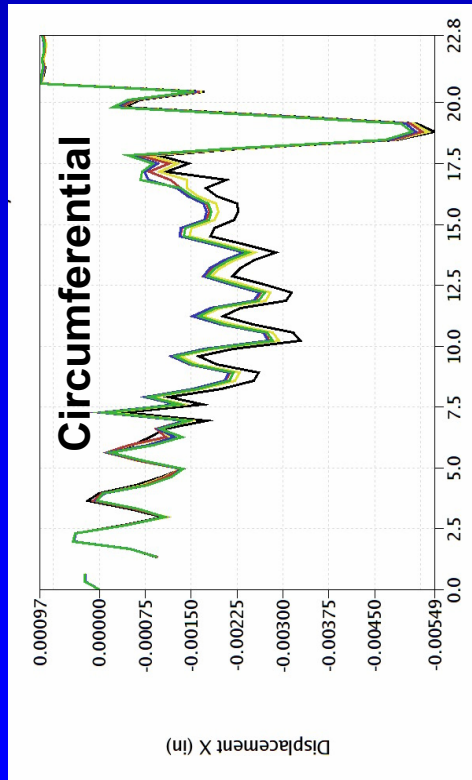
10kRPM, 5 psi



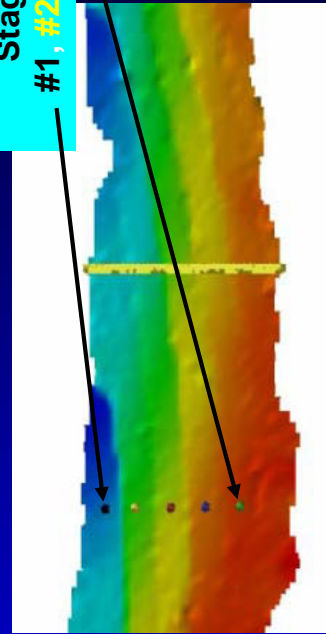
The
University
of Akron

FINGER BEHAVIOR WITH ROTATING SHAFT AND AXIAL PRESSURE DIFFERENTIAL $\Delta p=5$ PSI

Time History Displacement of The Stage Points



Stage points #1, #2, #3, #4, #5



The color of the stage points # corresponds to the color of the curves above

Time (sec)

November 8, 2005



CONCLUDING REMARKS (1)

Finger Behavior with Rotating Shaft and Axial Pressure Differential

Advanced
Technology



For Intelligent
Gas Turbines

- All the fingers vibrate because of the rotation of the shaft. Lifting force on the pad is very sensitive to the clearance between the pad and the shaft surface.
- In one coordinate direction, all the fingers move in the same manner
- At different radial locations, the x-displacement varies in the same manner
- The y- and z- displacements are different at different radial locations
- The z-displacement is smallest at the root of the fingers and at the back plate supporting point

November 8, 2005



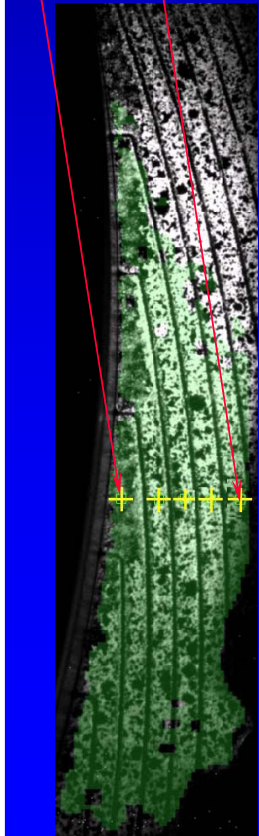
Advanced Technology



For Intelligent Gas Turbines

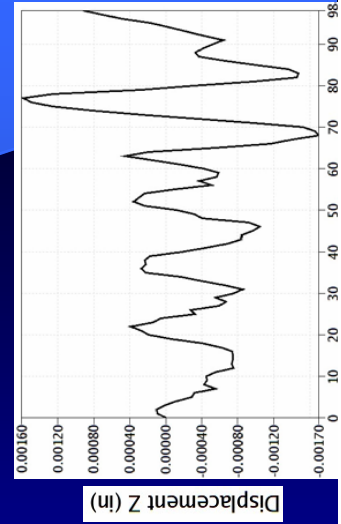
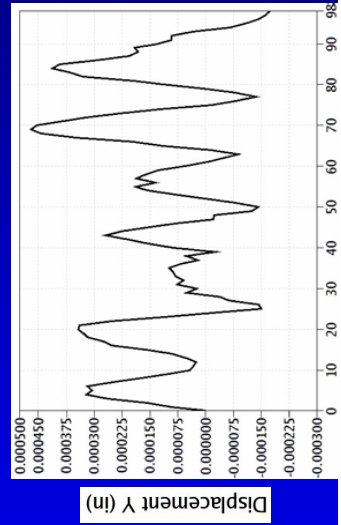
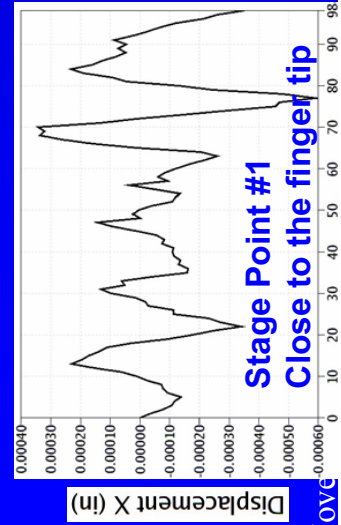
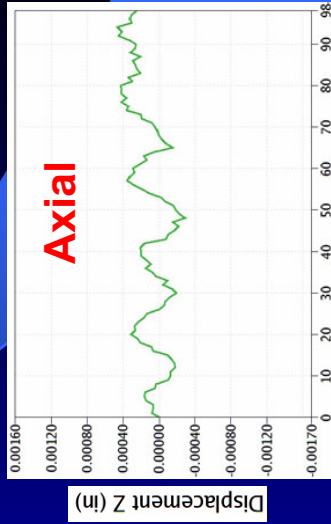
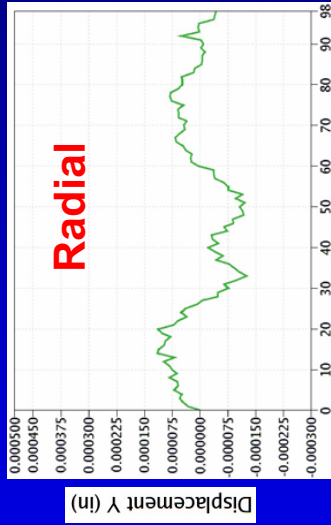
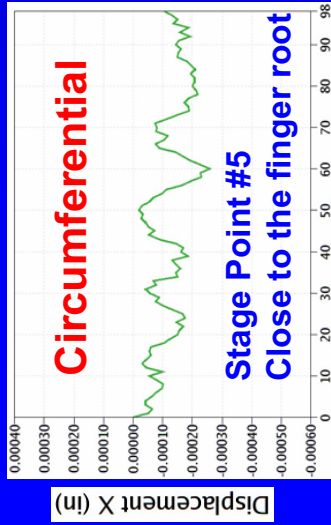
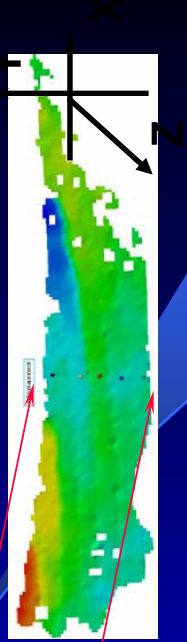
FINGER BEHAVIOR WITH ROTATING SHAFT

No Axial Pressure Differential



#1

#5



Nov



CONCLUDING REMARKS (2)

Finger Behavior with Rotating Shaft and No Axial Pressure Differential

Advanced
Technology



For Intelligent
Gas Turbines

- With the shaft rotating while no axial pressure drop, all the fingers move/vibrate independently. There is no phase correlation observed between the vibrations of the fingers.
- The displacement decreases from the finger tips to the finger roots
- At one location, the displacement magnitude of the vibration in three (x-, y-, z-) directions are roughly the same
- The movements of the fingers proved that all the fingers are lifted by the pressure build up under the bad due to the rotation of the shaft.

November 8, 2005



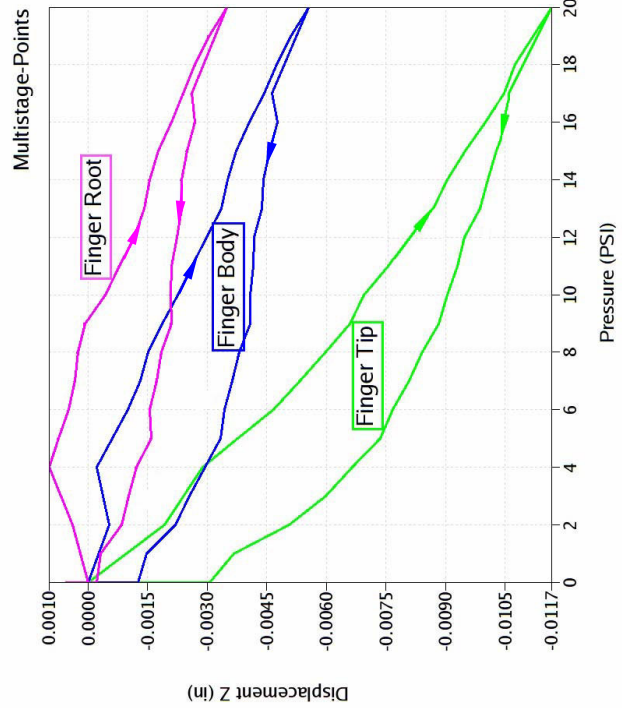
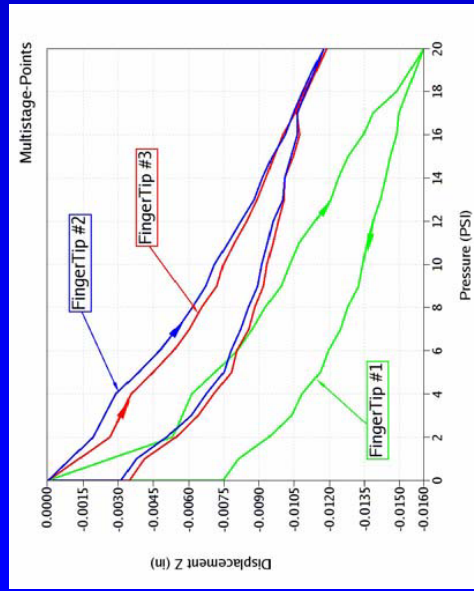
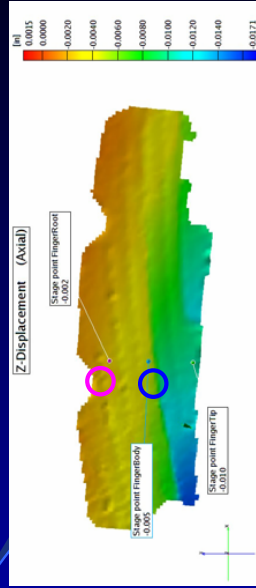
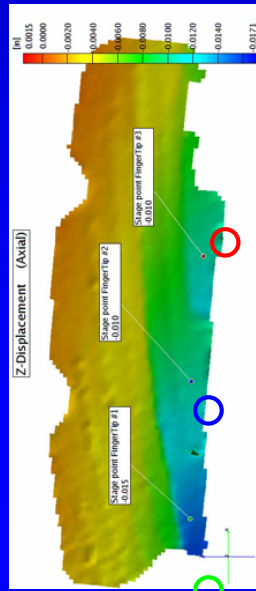
FINGER BEHAVIOR WITH AXIAL PRESSURE DIFFERENTIAL

Axial Pressure Shock: 0-20-0 PSI, No Shaft Rotation,

Advanced Technology



For Intelligent Gas Turbines



From initial state, pressure was increased from 0 to 20 psi and then decreased to 0 psi. The test was to investigate the finger behaviors under such a pressure shock

November 8, 2005



CONCLUDING REMARKS (3)

Finger Behavior with Axial Pressure Differential, No Shaft Rotation.

Advanced
Technology



For Intelligent
Gas Turbines

- With axial pressure drop only , all the finger moves in the same manner since all the fingers subject to roughly the same axial flow and axial pressure drop
- The deformation/bending of the fingers are three-dimensional.
- Displacement distributions shows sharp jump between the fingers, which indicates that they can move independently.

November 8, 2005

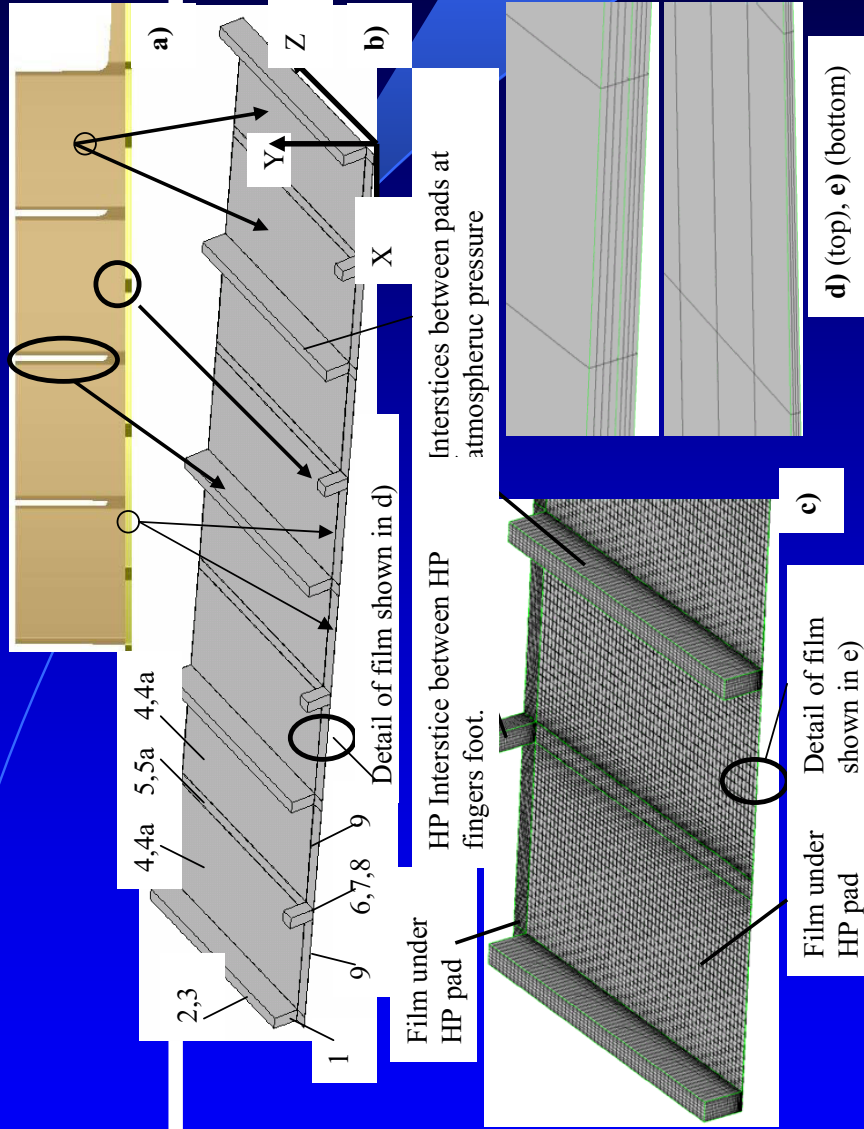


COMPUTATIONAL GRID

Advanced
Technology



For Intelligent
Gas Turbines



Grid Details for the Pressure, Flow and Temperature Calculations.

- a) Solid representation of the two rows of fingers viewed from below
- b) Corresponding representation of the fluid film contained between the rotor and the assembly of fingers.
- c) Detail of the cell structure in the fluid film below and in-between HP and LP pads.
- d) Fluid film grid structure under the HP finger
- e) Fluid film grid structure under the LP finger

November 8, 2005

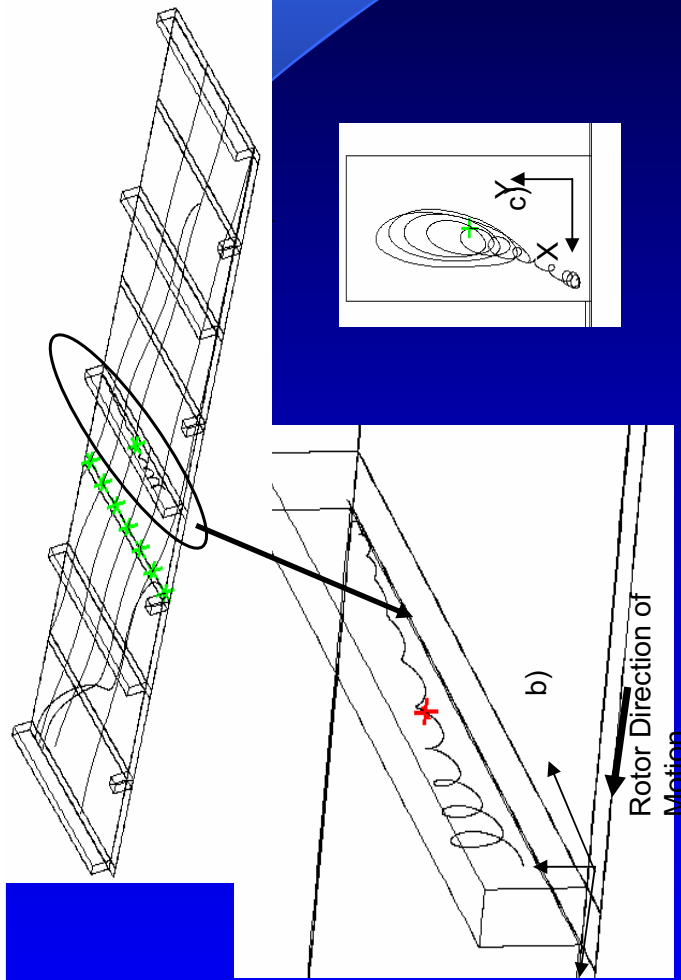


General 3-D Flow Patterns

Advanced
Technology



For Intelligent
Gas Turbines



Flow trajectories visualized with individual 4-finger cell showing circumferential flow. a) tracers showing circumferential flow; b) 3-D flow between low pressure fingers, c) frontal view of flow in b)

November 8, 2005

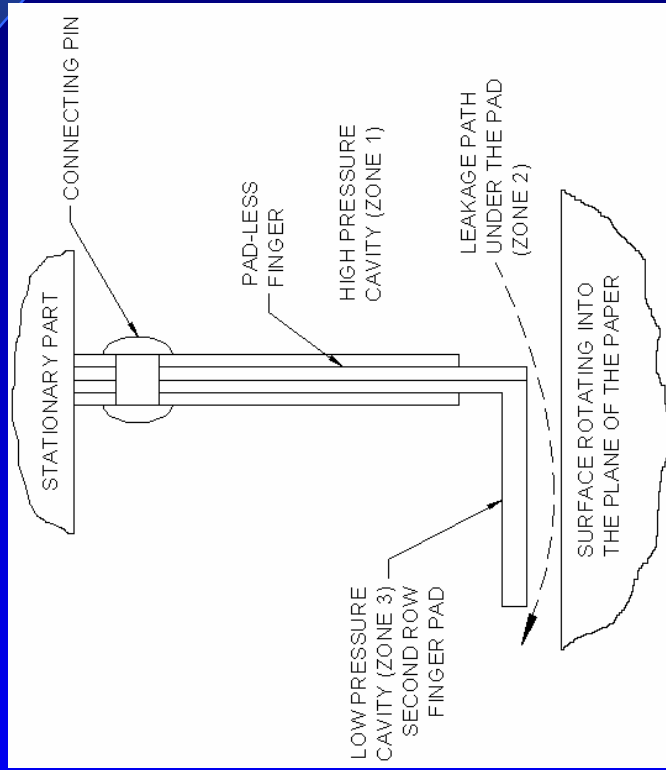


THERMOFLUID BOUNDARY CONDITIONS

Advanced Technology



For Intelligent Gas Turbines



Boundary conditions for the Finger Seal. Schematic Cross Section with Two Rows of Padded Low- and Pad-less High Pressure Fingers

November 8, 2005

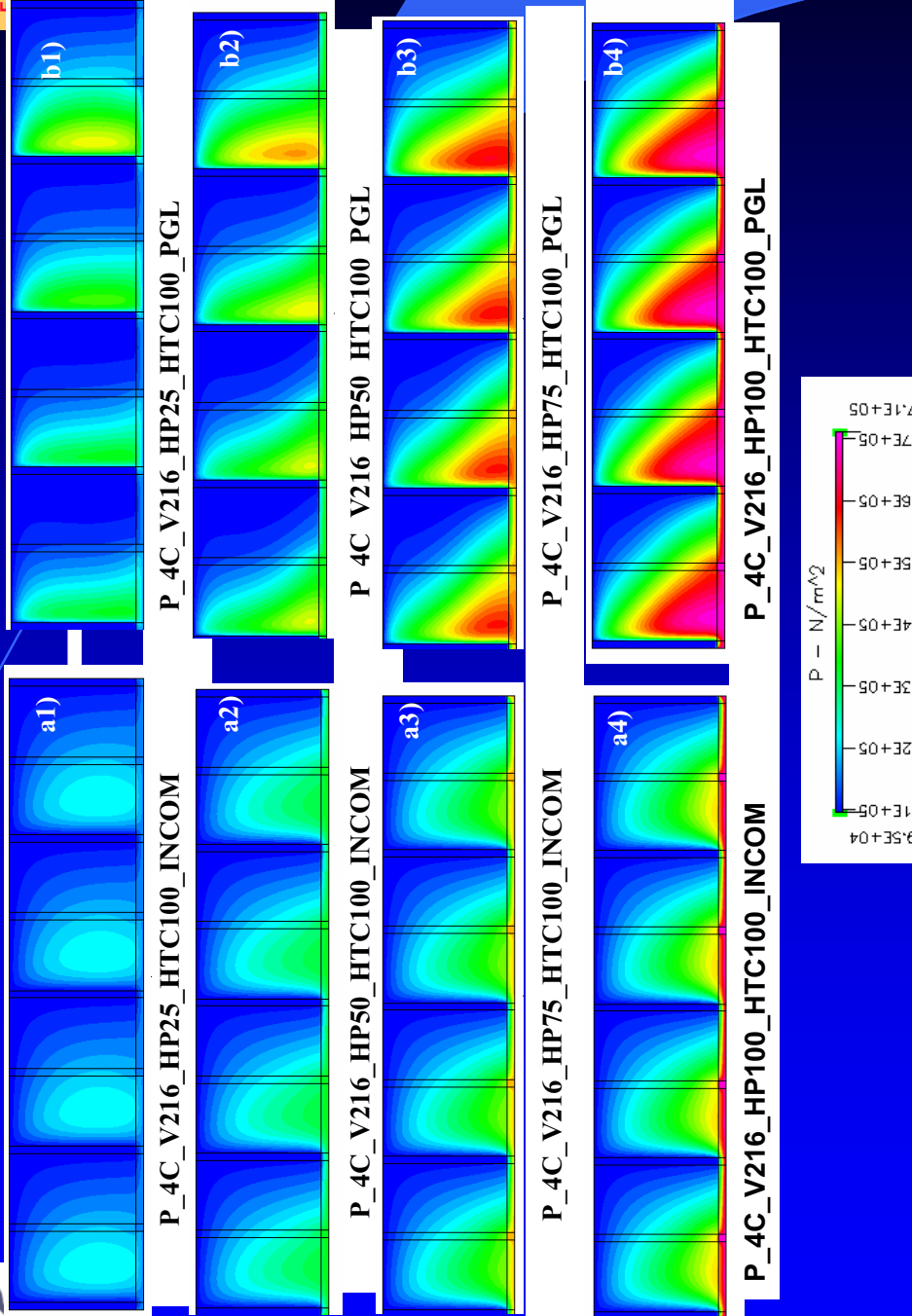


PRESSURES: INCOMPRESSIBLE vs. PGL

Advanced Technology



For Intelligent Gas Turbines



Comparison between pressure magnitude development under the fingers when incompressible ($\rho, \mu = \text{const}$) and perfect gas laws are used.

November 8, 2005

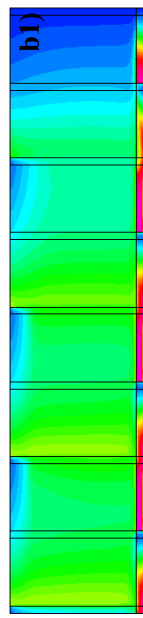
TEMPERATURES: INCOMPRESSIBLE VS. PGL



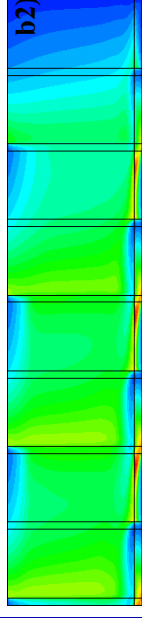
Advanced
Technology



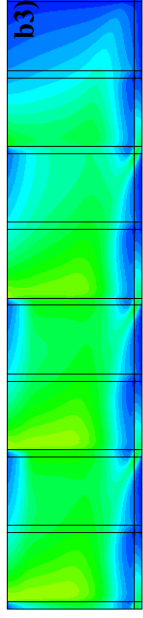
For Intelligent
Gas Turbines



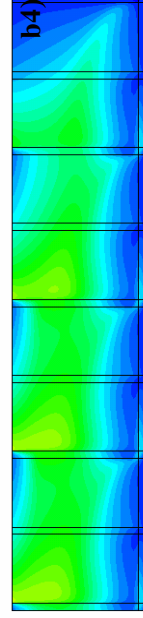
T_4C_V216_HP25_HTC100_INCOM



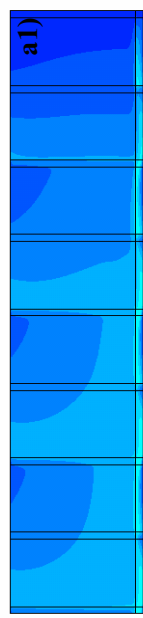
T_4C_V216_HP50_HTC100_INCOM



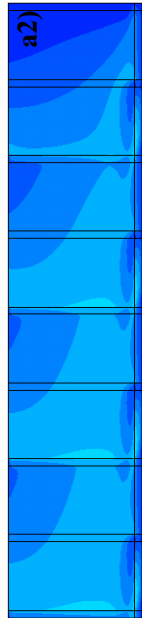
T_4C_V216_HP75_HTC100_INCOM



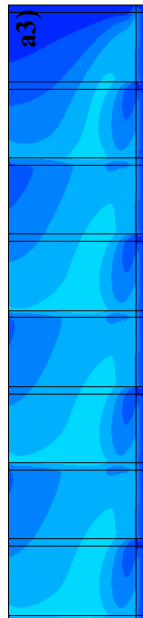
T_4C_V216_HP100_HTC100_INCOM



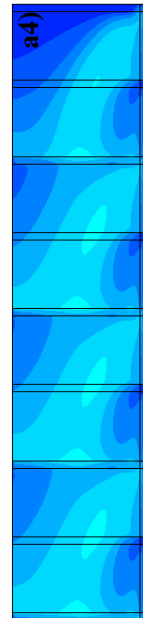
T_4C_V216_HP25_HTC100_PGL



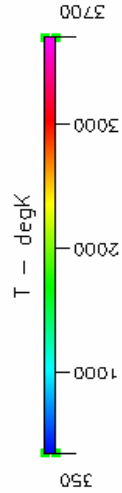
T_4C_V216_HP50_HTC100_PGL



T_4C_V216_HP75_HTC100_PGL



T_4C_V216_HP100_HTC100_PGL



Comparative temperature map for the incompressible and perfect gas law cases. The adiabatic case.

November 8, 2005

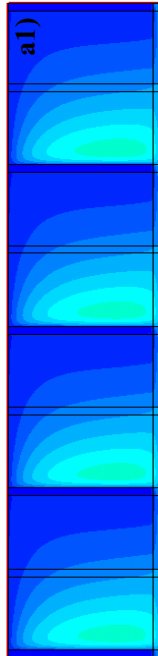


PRESSURES: ISOTHERMAL 216 m/s and 432 m/s

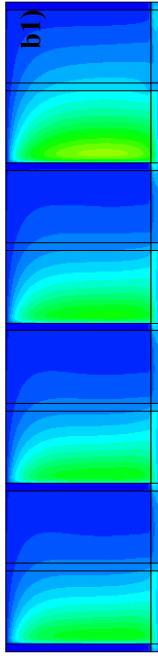
Advanced
Technology



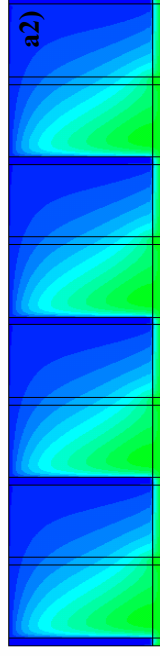
For Intelligent
Turbines



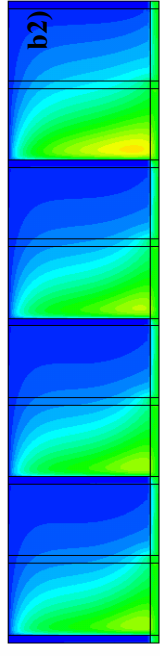
P_4C_V216_HP25_HTC1000_PGL



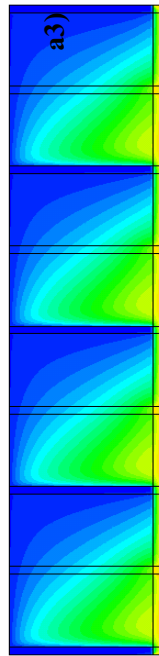
P_4C_V432_HP25_HTC1000_PGL



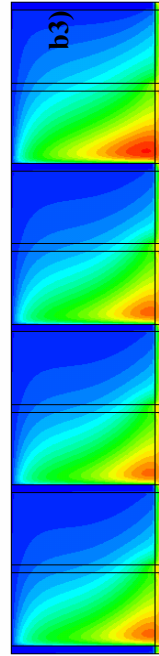
P_4C_V216_HP50_HTC1000_PGL



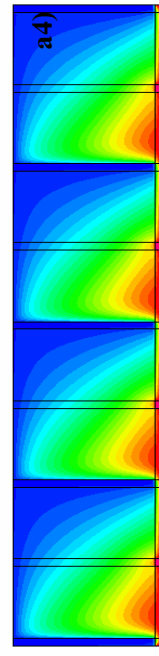
P_4C_V432_HP50_HTC1000_PGL



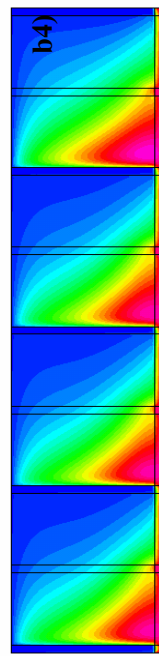
P_4C_V216_HP75_HTC1000_PGL



P_4C_V432_HP75_HTC1000_PGL



P_4C_V216_HP100_HTC1000_PGL

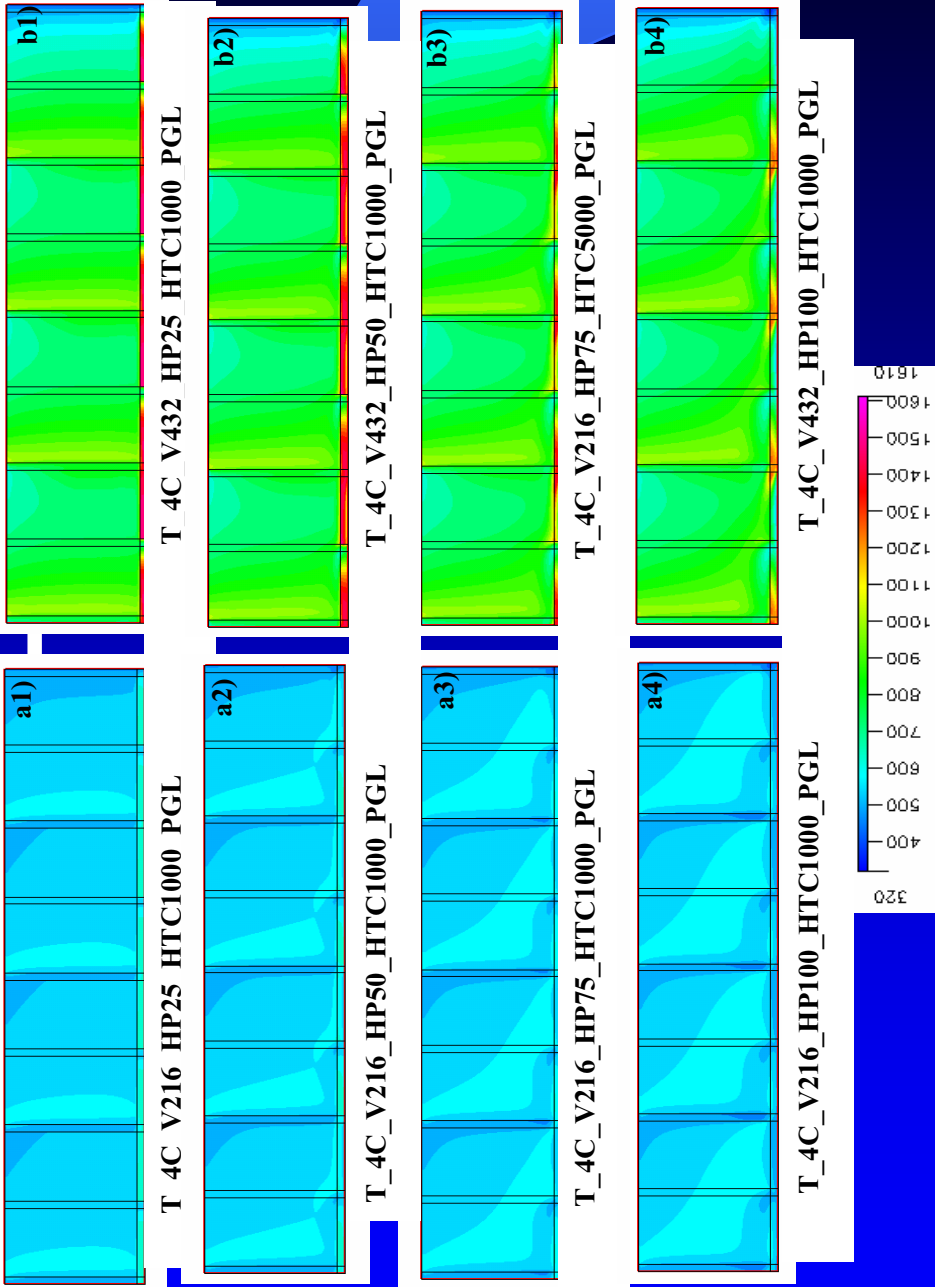


P_4C_V432_HP100_HTC1000_PGL

Comparison between pressure profiles when the linear velocity of the rotor is increased from 216 m/s to 432 m/s. The isothermal case.

November 8, 2005

TEMPERATURES: ALMOST ISOTHERMAL (1000 W/m²K) 216 m/s and 432 m/s



Temperature development when the angular velocity is varied from 216 m/s linear, to 432. The almost isothermal case.

November 8, 2005

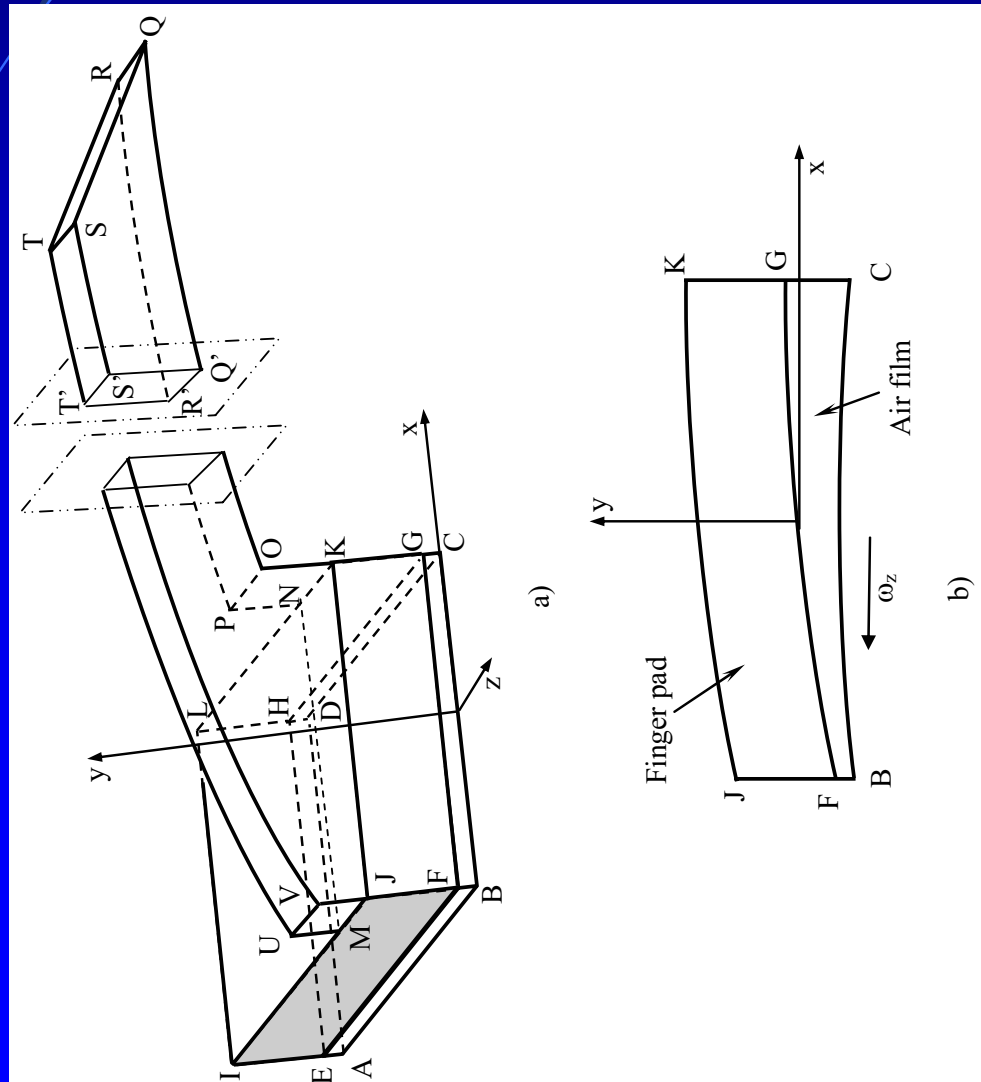


Single Finger Geometry (Solid-Fluid Interaction)

Advanced
Technology



For Intelligent
Gas Turbines



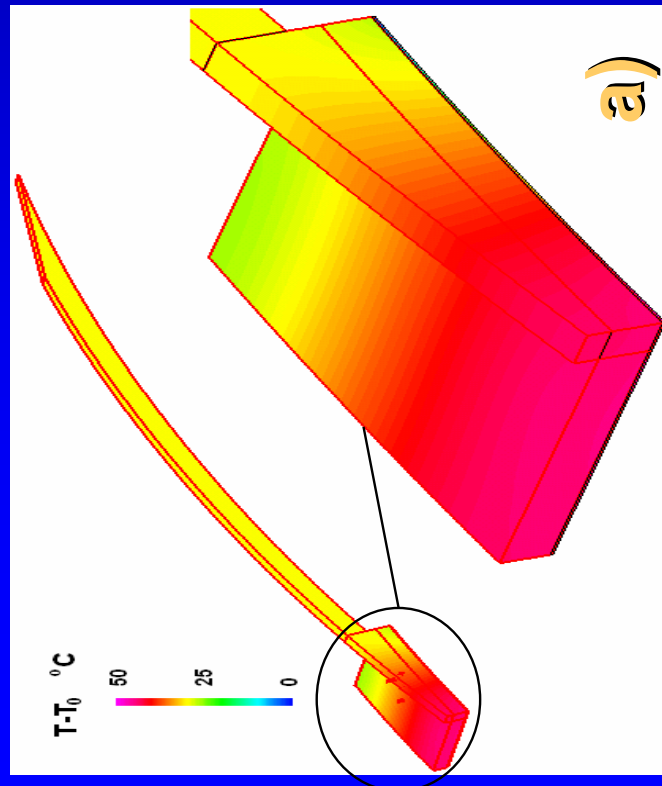


Moving Finger

Advanced
Technology

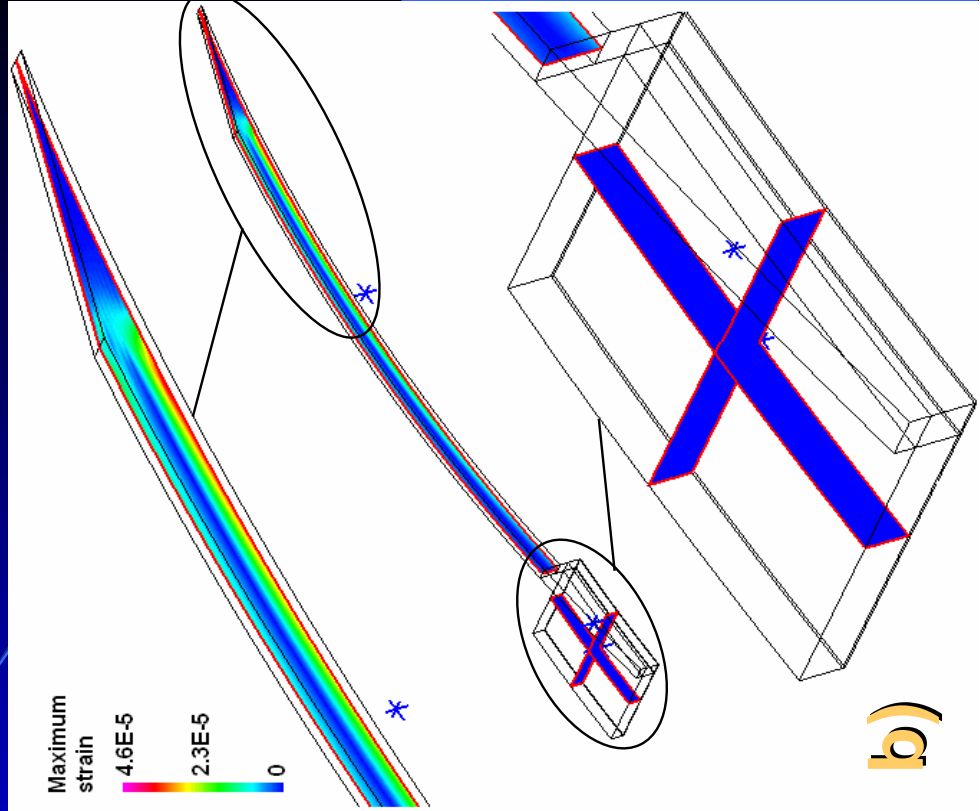


For Intelligent
Gas Turbines



Temperature (a) and strain (b) in the finger pad and leg. Adiabatic conditions on finger and rotor surfaces.

Rotor rotates at 30000 rpm



November 8, 2005

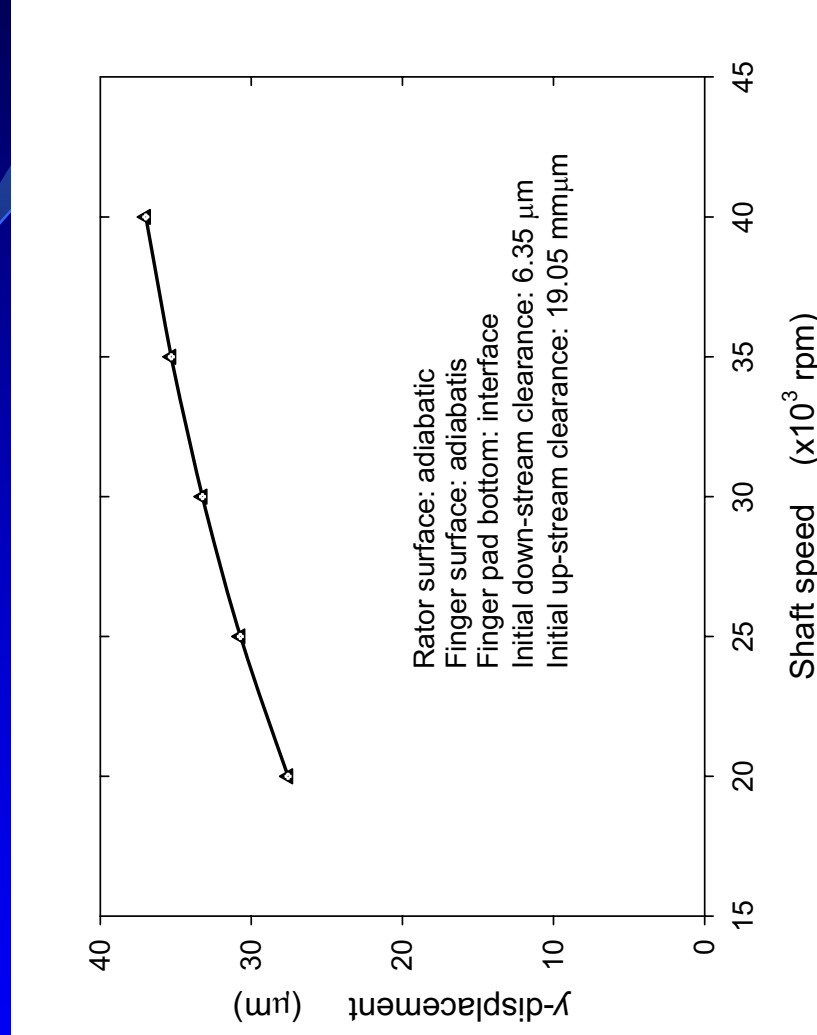
Lift of the pad central section with angular velocity



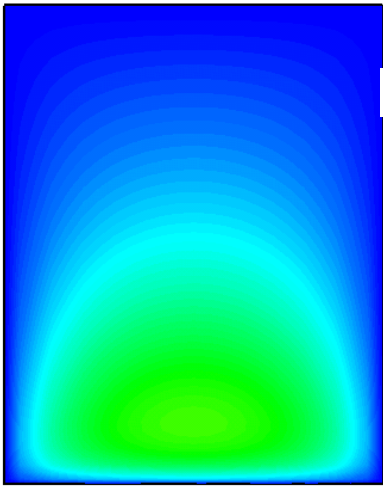
Advanced
Technology



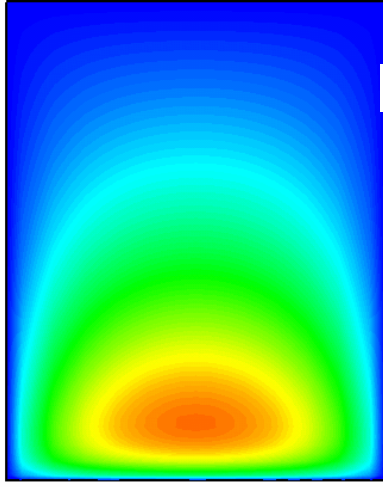
For Intelligent
Gas Turbines



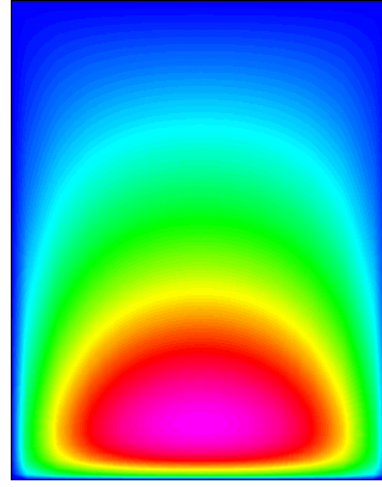
November 8, 2005



20,000 rpm



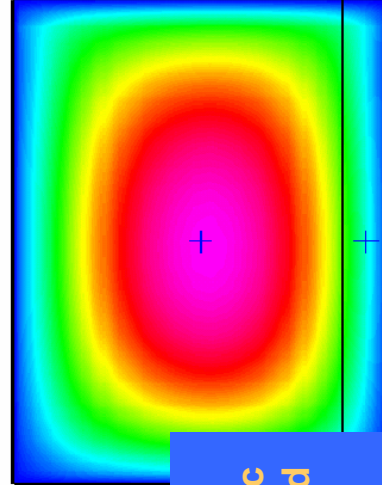
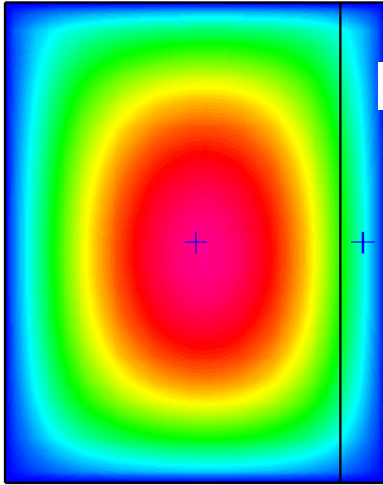
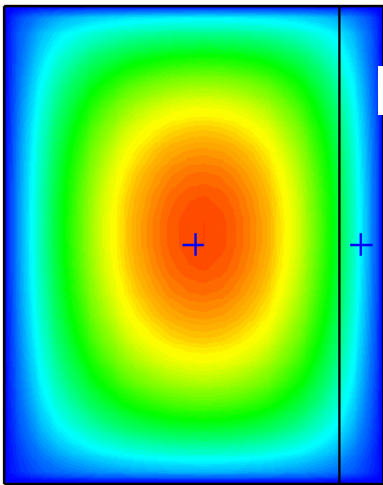
30,000 rpm



40,000 rpm

Pressure $\frac{N}{m^2}$
 4.2E5
 2.1E5
 0

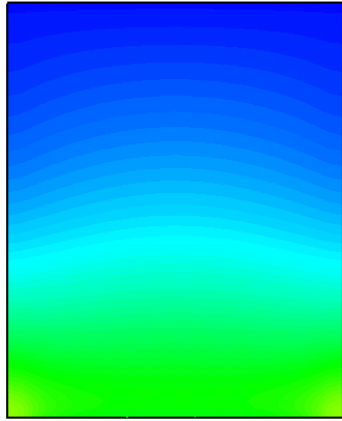
Pure Hydrodynamic Pressure build up under the rigid finger



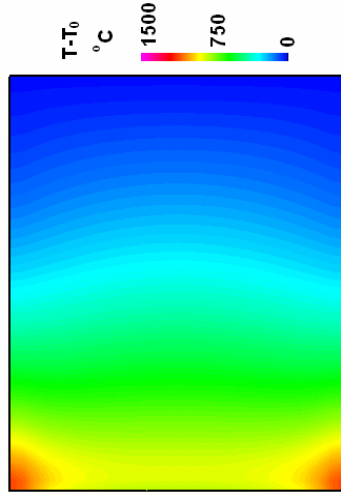
Pressure $\frac{N}{m^2}$
 1600
 800
 0

Pure Hydrodynamic Pressure build up under the lifting finger

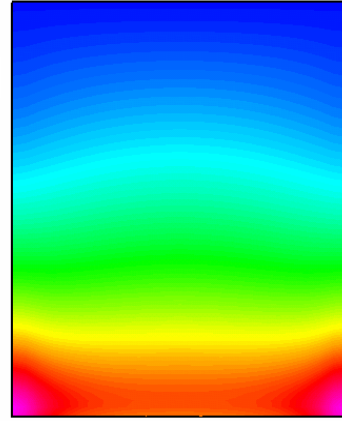




a')

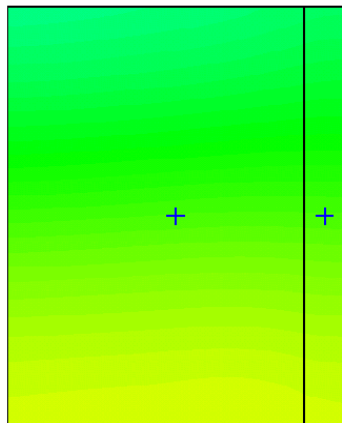


b')

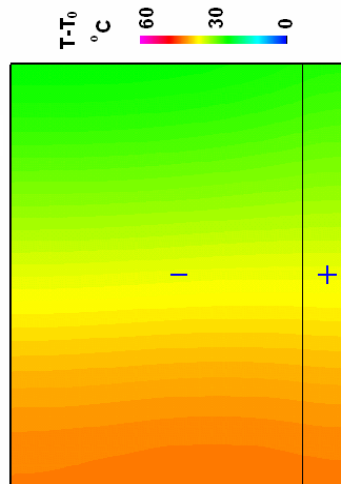


c')

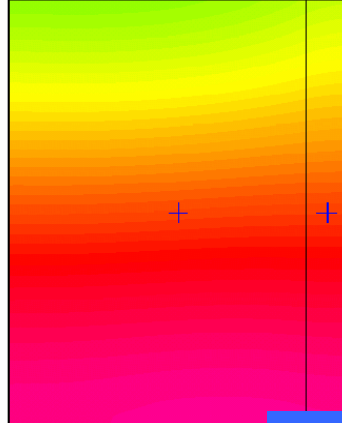
Pure Hydrodynamic Temperature build up under the **rigid** finger



a)



b)



c)

Pure Hydrodynamic Temperature build up under the **lifting** finger

Rotor and pad upper surface are adiabatic. The pad itself allows 3-D energy transfer

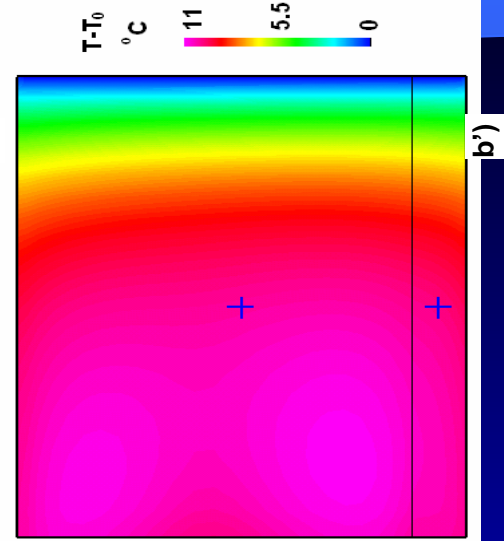
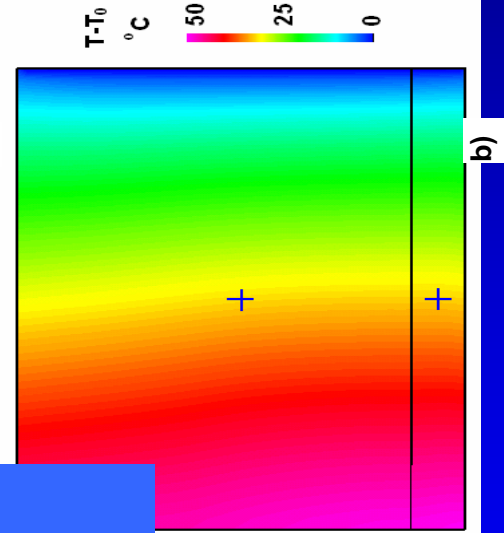
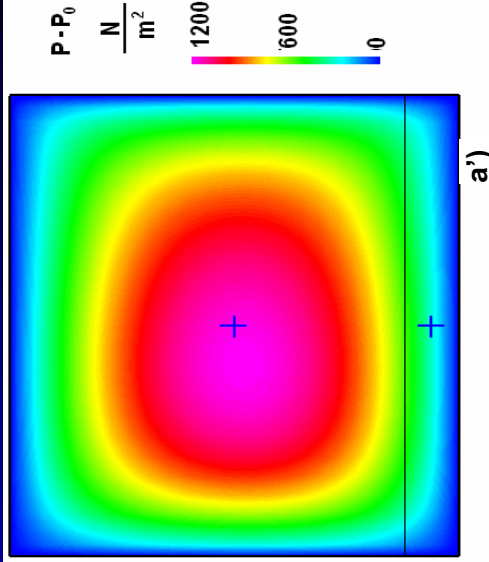
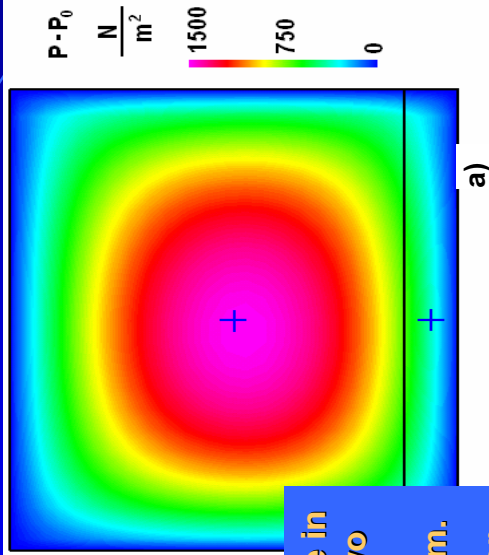


Comparison between adiabatic and thermal conditions

Advanced Technology

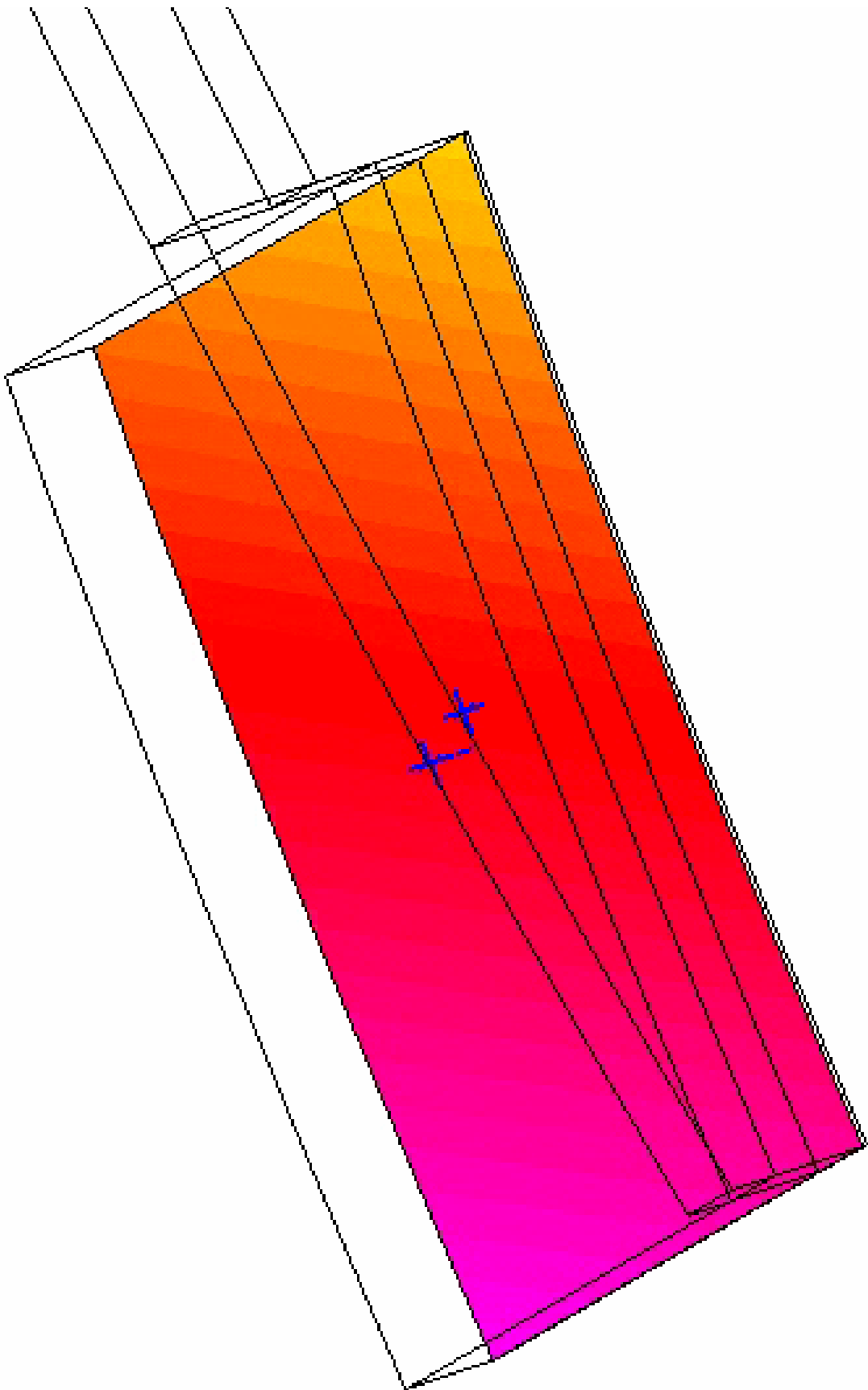


For Intelligent Gas Turbines



The pressure and temperature in the center of the air film for two thermal boundary conditions with rotor rotating at 30000 rpm. (a, b) Adiabatic rotor and finger surfaces. (a', b') Isothermal rotor and finger surfaces at T_0 .

November 8, 2005



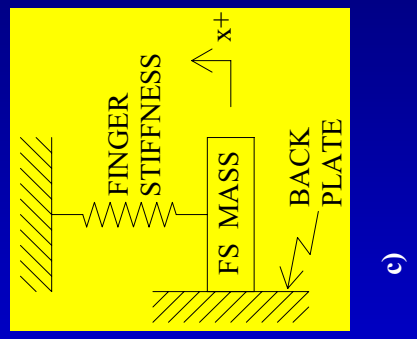
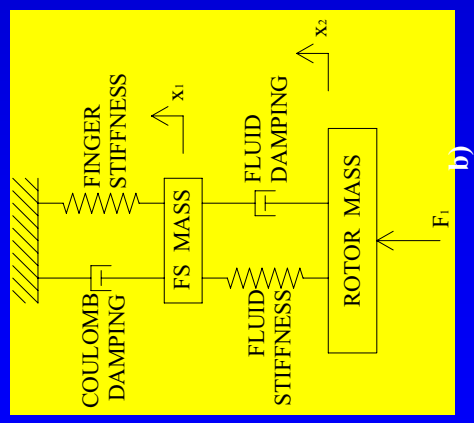
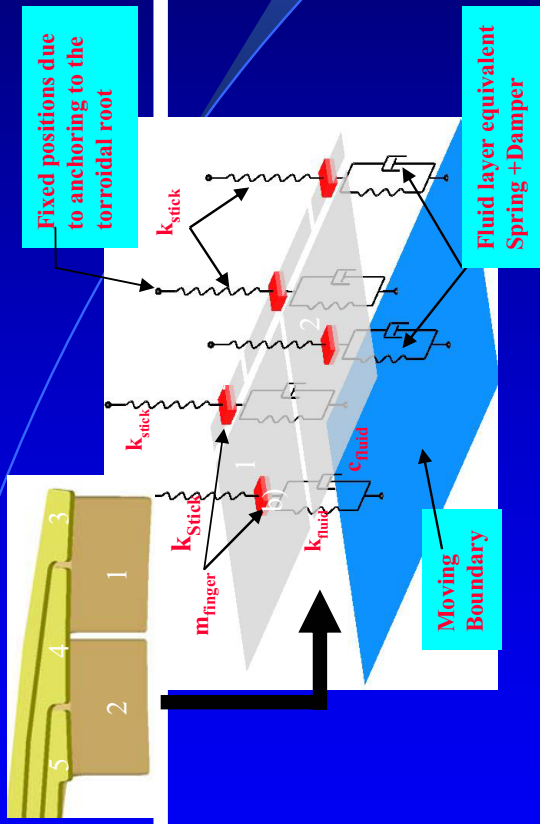


EQUIVALENT DYNAMIC MODEL

Advanced Technology



For Intelligent Gas Turbines



Solid model and Equivalent Spring-Mass-Spring/Damper representation for use in the equation of motion simulation
November 8, 2005



FINGER DYNAMICS-2

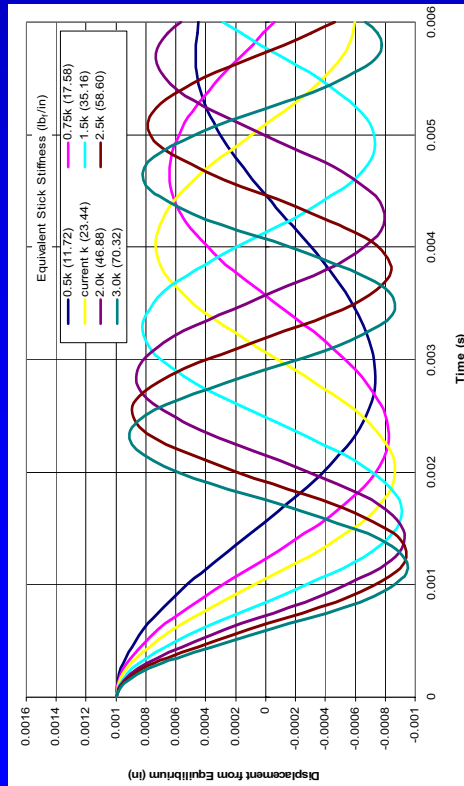
Free Vibration

Stiffness is varied

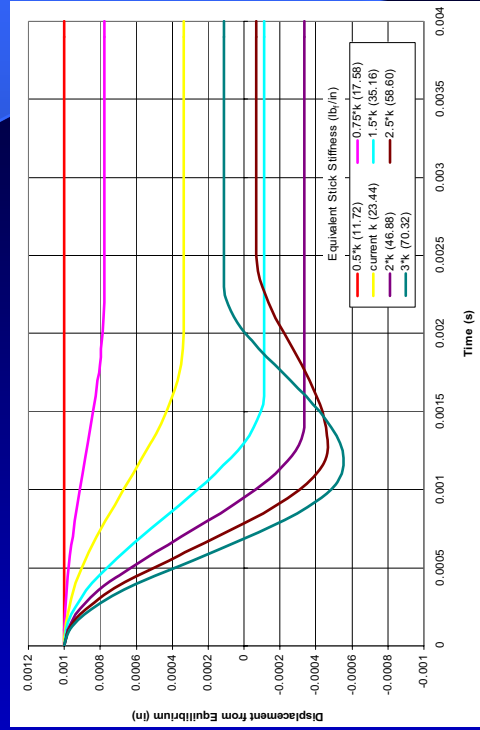
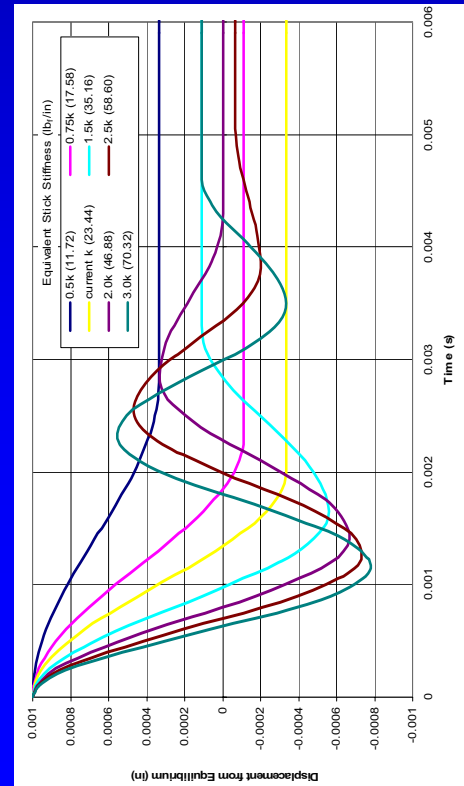
Advanced
Technology



For Intelligent
Gas Turbines



Finger assembly free vibration when k_{Stick} is varied:
 a) $\Delta p_C = 6.9$ kPa (1psi); b) $\Delta p_C = 34.5$ kPa (5psi); c)
 $\Delta p_C = 69$ kPa (10psi);



November 8, 2005

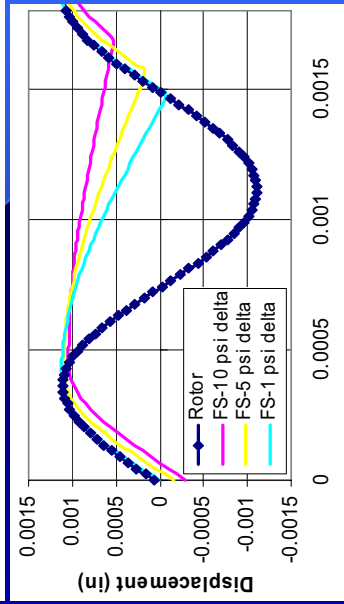
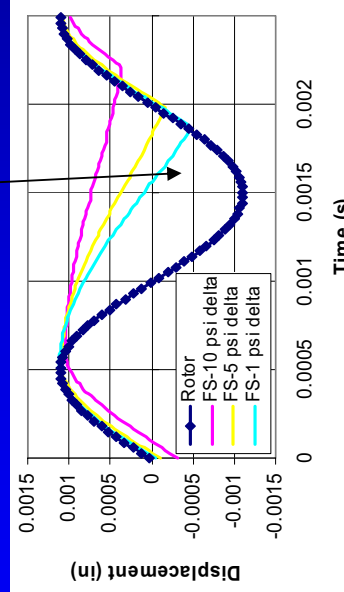
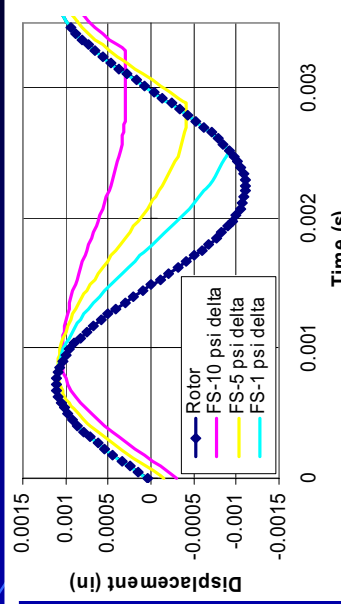
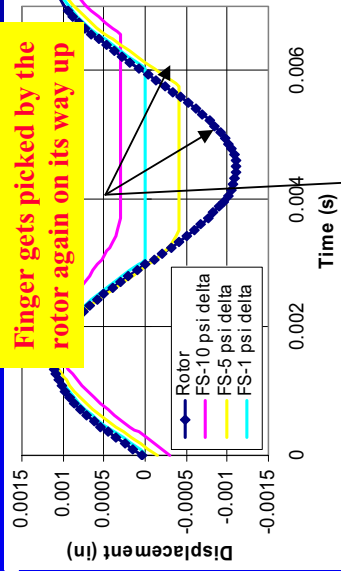


FINGER DYNAMICS

Advanced
Technology



For Intelligent
Gas Turbines



Finger following the rotor when Coulomb damping force and rotor angular velocity is varied. Finger stiffness is

$$k_{Seqm} = 3.58 \frac{N}{m} \left(20.44 \frac{lbf}{in} \right);$$

- a) 10,000 rpm (108 m/s); b) 20,000 rpm (216 m/s); c) 30,000 rpm (324 m/s); d) 40,000 rpm (432 m/s)

November 8, 2005



SOME EXPERIMENTAL WORK

November 8, 2005



DIAGRAMS OF THE TEST SECTION

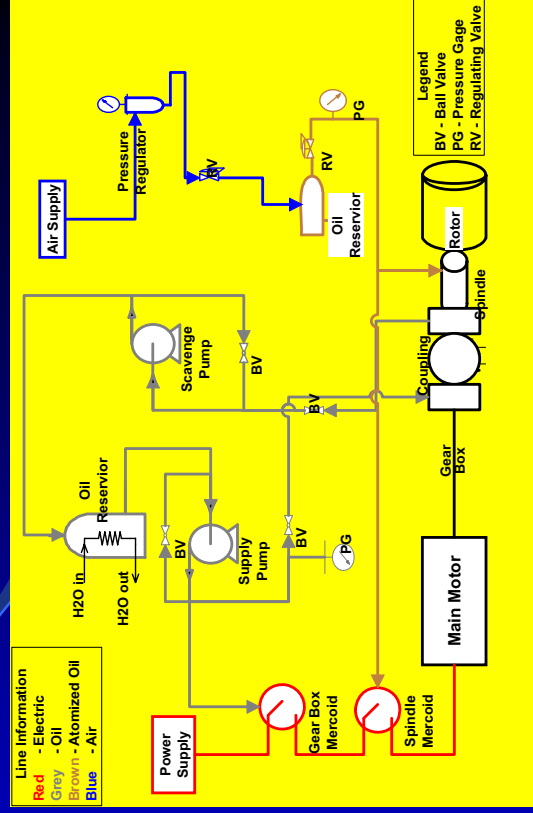
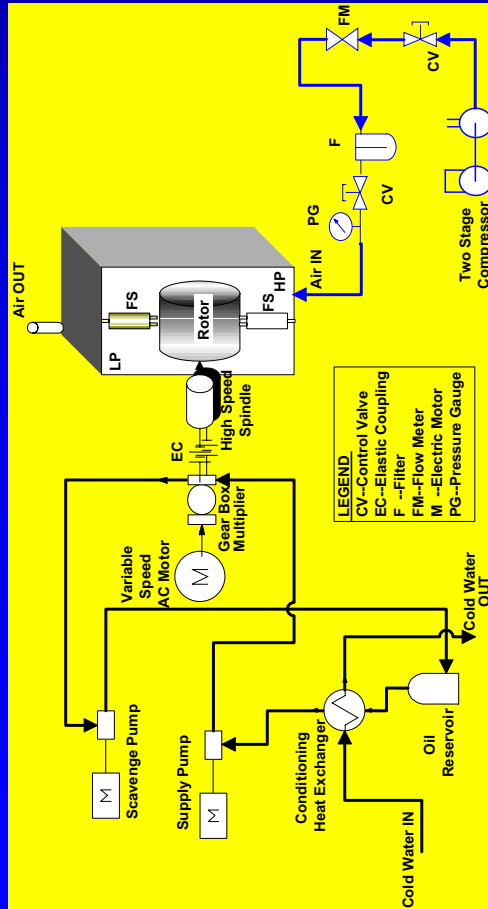
Overall Installation

Electric, Oil and Air Circuits

Advanced Technology



For Intelligent Gas Turbines



Overall Installation

Electric, Oil and Air Circuits

November 8, 2005



EXPERIMENTAL INSTALLATION

Advanced
Technology



For Intelligent
Gas Turbines



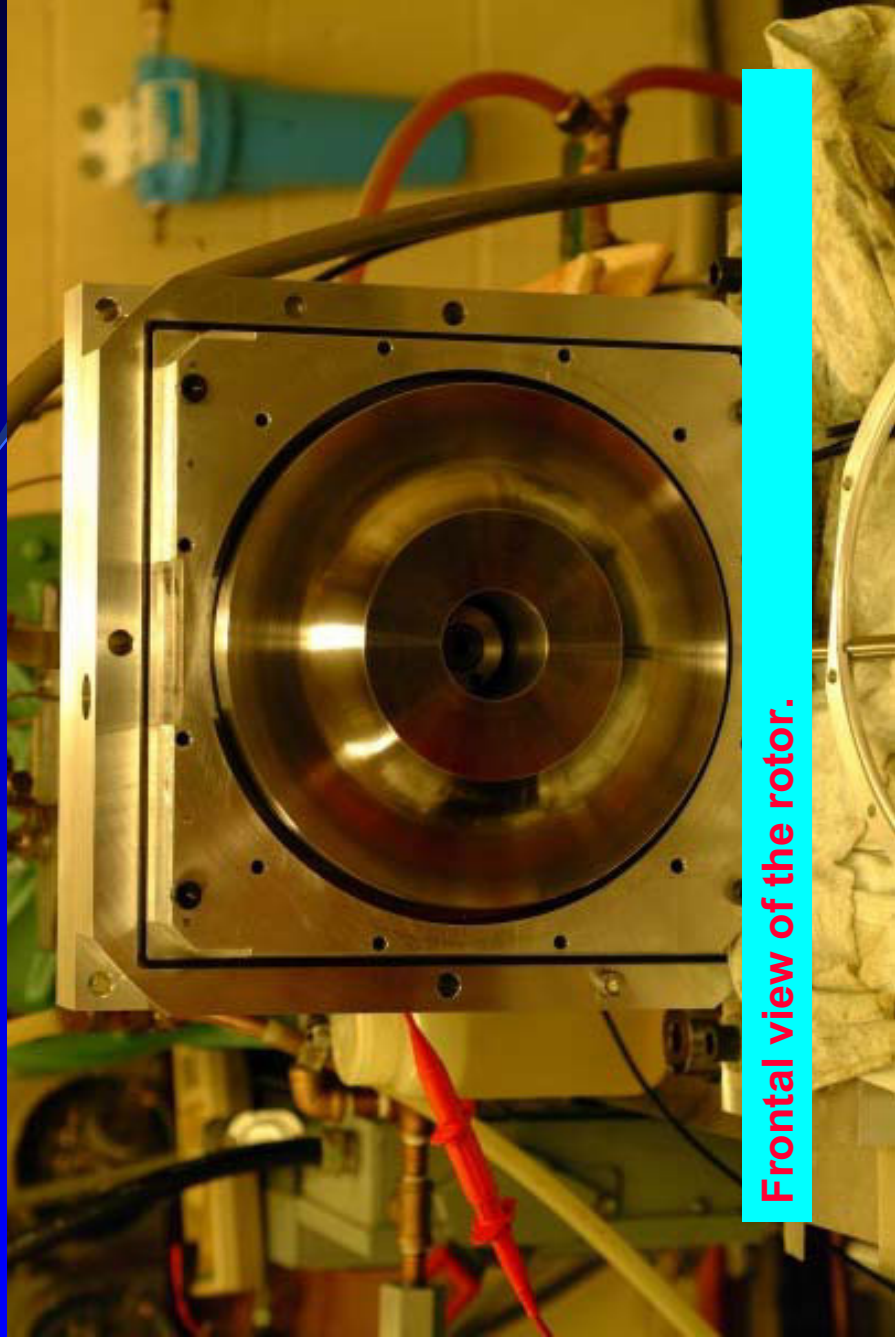
Drive Train



Rotor Section

November 8, 2005

ROTOR: FRONTAL VIEW



Frontal view of the rotor.

November 8, 2005

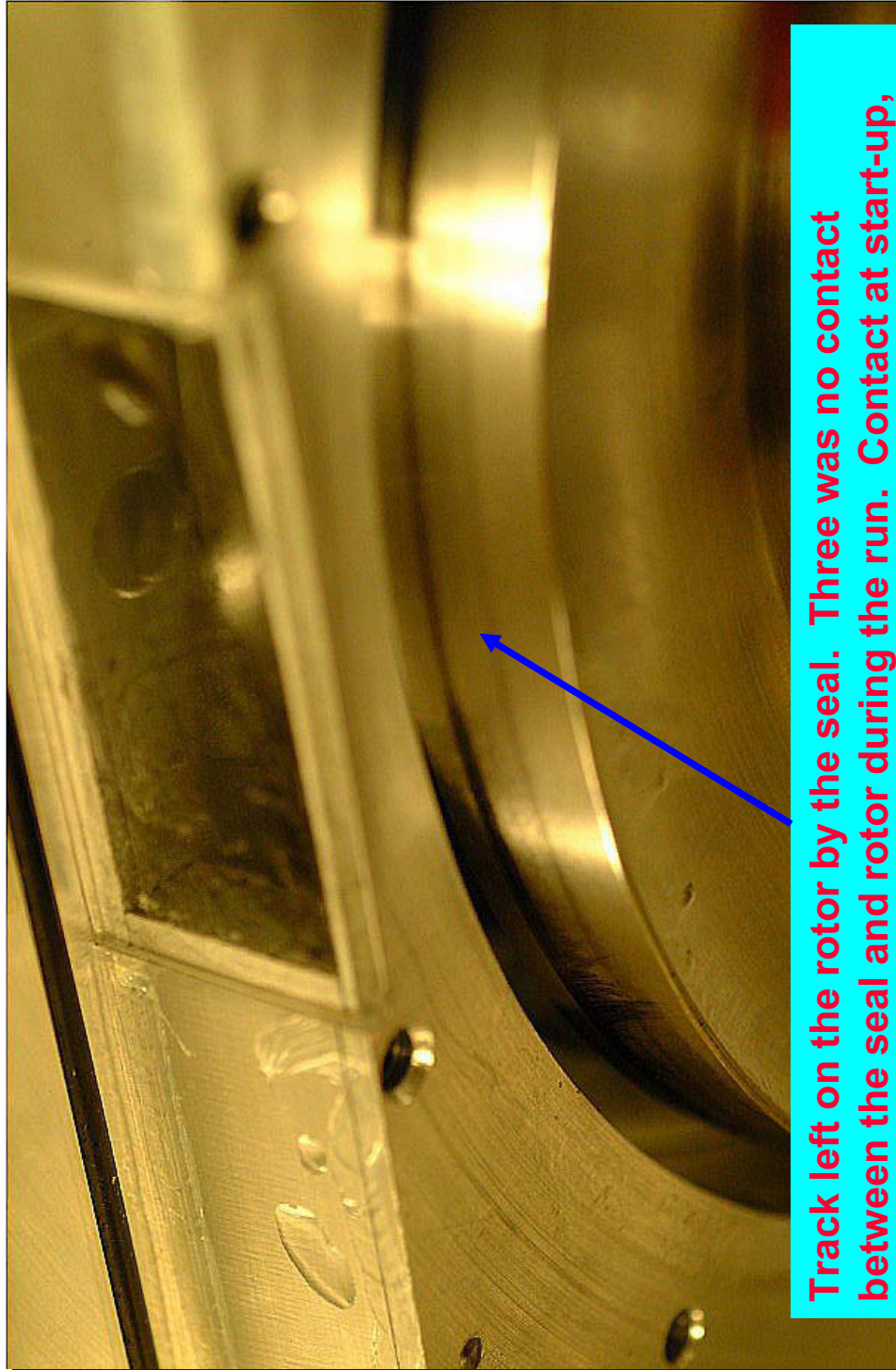
ROTOR SURFACE



Advanced
Technology



For Intelligent
Gas Turbines



Track left on the rotor by the seal. Three was no contact between the seal and rotor during the run. Contact at start-up, liftoff-no contact, contact again at coast-down

November 8,

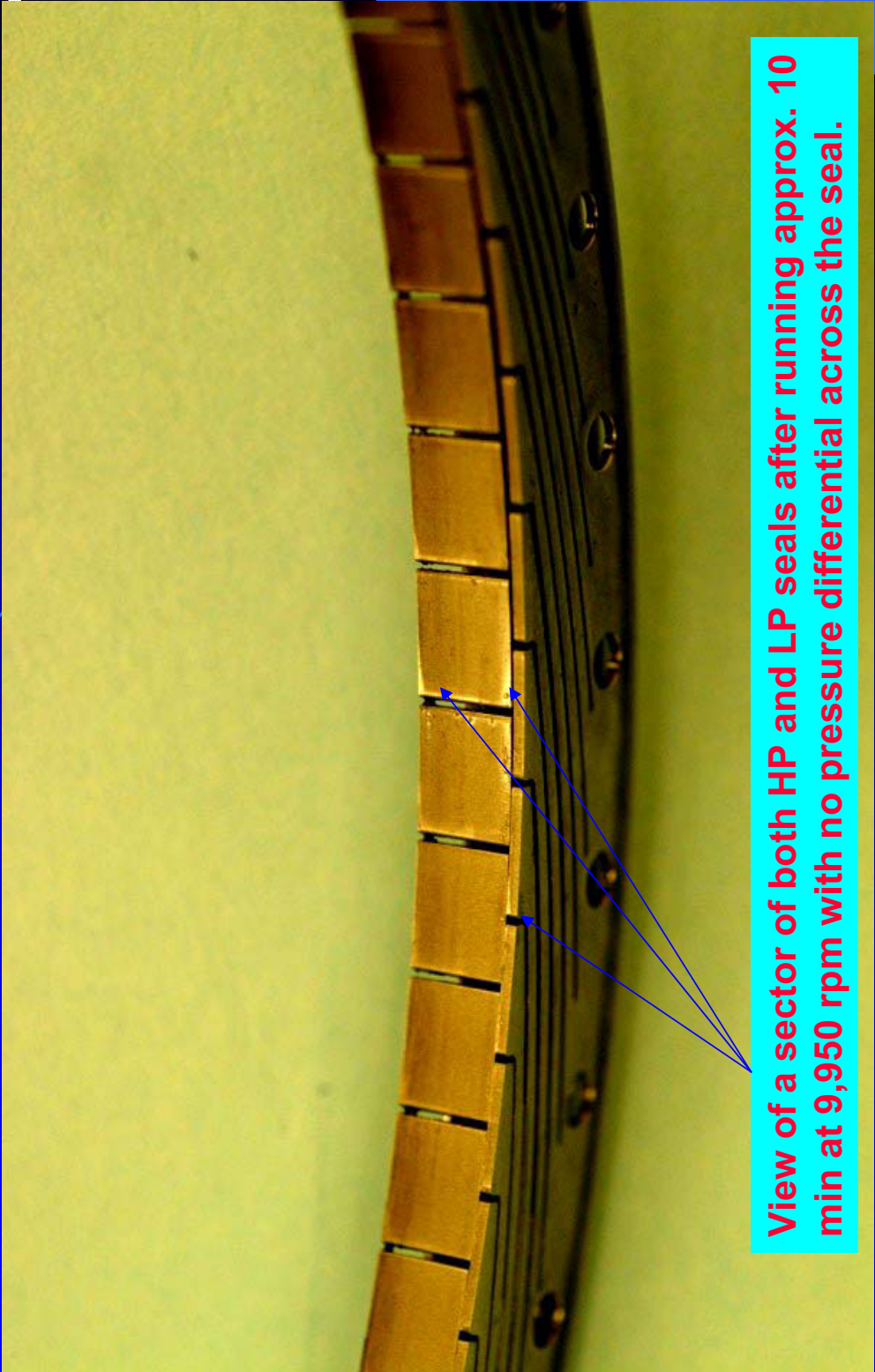


FINGERS' PAD UNDERSURFACE

Advanced
Technology



For Intelligent
Gas Turbines



View of a sector of both HP and LP seals after running approx. 10 min at 9,950 rpm with no pressure differential across the seal.

November 8, 2005



FINGERS' PAD UNDERSURFACE DETAILS

Advanced
Technology



For Intelligent
Gas Turbines

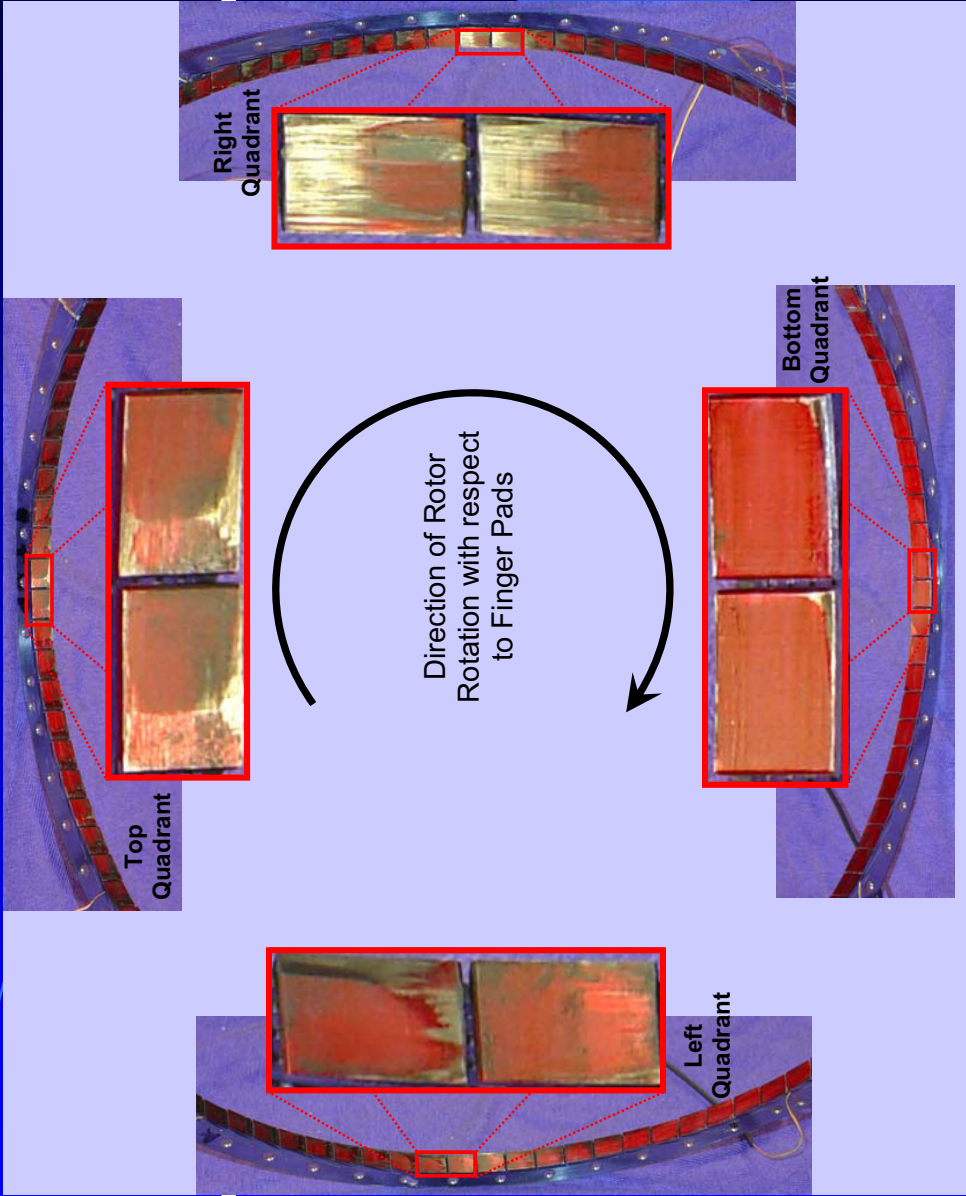
Slight traces of
wear



HP side

Enlarged view of two pads after the 10 min. run

November 8, 2005



LP Finger Underside Pads Surface Showing Ink Wear Marks after a Total Run Time of 97 min at a nominal speed of 9,950 rpm; This included 4 start-ups and 4 coast-downs. Seal Quadrants Positioned as Viewed from the Low-Pressure Side

November 8, 2005

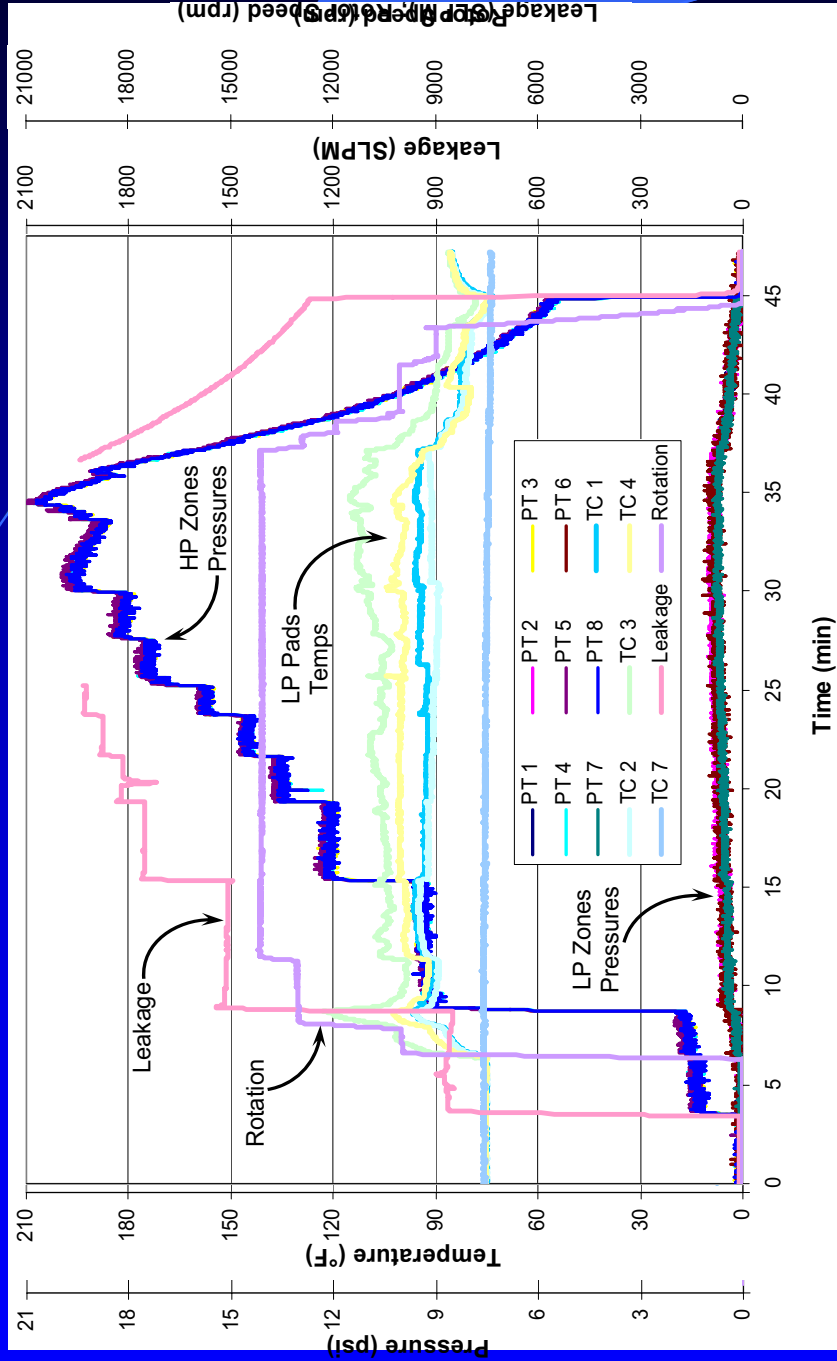


LEAKAGE FLOW PERFORMANCE SUPERIMPOSED ON ROTATION, TEMPERATURE AND PRESSURE DIFFERENTIAL

Advanced
Technology



For Intelligent
Gas Turbines



November 8, 2005



FLOW FACTOR vs. PRESSURE DIFFERENTIAL

